# Population coding of pattern separation in the monkey hippocampus

John J. Sakon & Wendy A. Suzuki

Center for Neural Science, New York University, 4 Washington Place, New York, NY 10003.

Correspondence: john@cns.nyu.edu or wendy@cns.nyu.edu

## Abstract

The CA3 and dentate gyrus (DG) regions of the hippocampus are considered key for disambiguating sensory inputs from similar experiences in memory, a process termed pattern separation. The neural mechanisms underlying pattern separation, however, have been difficult to compare across species: rodents offer robust recording methods with less human-centric tasks while humans provide complex behavior with less recording potential. To overcome these limitations, we trained monkeys to perform a visual pattern separation task similar to those used in humans while recording activity from single CA3/DG neurons. Using a novel looking pattern assay to evaluate behavior, we find that when animals distinguish recently seen novel images from similar images, indicative of pattern separation, CA3/DG neurons treat the similar images more like novel than repeat images. Further, while many hippocampal neurons respond during pattern separation, only a limited proportion respond to any given pattern separation event, consistent with a sparse distributed code.

## Introduction

Pattern separation is the putative process the brain uses to differentiate similar inputs into non-overlapping outputs[1,2]. In the case of memory, when a subject is shown an image similar to one they recently viewed, pattern separation mechanisms are tasked to differentiate the newly presented image from their memory of similar images. Experimental work has found that the CA3 and dentate gyrus (CA3/DG) regions of the hippocampus show neurophysiological signals correlated with successful mnemonic pattern separation in humans[3-7] and rats[8-12].

However, there remain key gaps in our understanding of the neural basis of pattern separation from this cross-species literature. For example, human fMRI studies revealed BOLD responses in the CA3/DG regions of hippocampus characteristic of pattern separation[3-6] but are limited by spatial and temporal resolution of the BOLD signal. Important studies in rodents have shown electrophysiological correlates of pattern separation of spatial environments in populations of CA3/DG neurons[8-11], but the differences between the experimental designs used across human and rodent studies make these results difficult to compare. In particular, other than the usual difficulties in comparing BOLD with single neuron responses[13], human pattern separation tasks typically involve discrimination of visual stimuli from memory on timescales less than 1 second[3,4,6,7,14], while rodent pattern separation tasks involve spatial discrimination of environments over the course of minutes[9-12].

Here we address this gap between human and rodent pattern separation work by electrophysiologically recording from single neurons in the CA3/DG regions of the monkey hippocampus as animals perform a visual pattern separation task closely related to that used in human fMRI work[3]. The use of non-human primates gives us the ability to perform single unit recording while quantifying the relatively complicated behavior required to assess pattern separation on a trial-by-trial basis. In particular, the combination of these techniques allow us to address the hypothesis—suggested by human fMRI work[3,4,6]—that CA3/DG neurons maintain similar firing rates (firing rates) in response to novel and similar images when animals succeed in behavioral pattern separation but respond differentially to novel and repeat images during successful recognition. We also investigate if pattern separation is driven by a subset of CA3/DG neurons or through varying levels of contribution from the whole population. Finally, we ask if hippocampal regions CA3/DG show stronger signals for pattern separation or recognition memory.

## Results

**Behavior**: The behavioral task we used was closely modeled after a paradigm used in humans to examine pattern separation in the hippocampus with fMRI[3]. In this task, monkeys serially viewed three categories of images: **Novel** images, which the animal had never seen before; **Lure** images, which had strong visual similarity to a previously seen novel image (examples shown in Fig. S1); and **Repeat** images, which were exact replicas of a previously seen novel image (Fig 1A). Lure and repeat images were shown within 0-3 trials after their respective novel image was

shown. Animals were allowed to look at each image as long as desired (up to 10 s) until they ended the trial by saccading outside the bounds of the image. We compiled 19,350 novel images, 6450 repeat images (each a repeat of an image from the novel set) and 6450 lure images (each similar to an image from the novel set). In this way, monkeys never saw any novel or lure image more than once or the repeated novel image more than twice.

We utilized a preferential looking framework to gauge the monkeys' ability to identify repeat and lure images[15,16]. To assess animals' overall performance on the task, we pooled the looking times for each of the three trial types for 121 sessions in three macaque monkeys (Rhesus BY=55 sessions, Rhesus I=56 sessions, Bonnet B=10 sessions). Consistent with previous studies in monkeys[15] and infants[16], we found that animals looked for significantly less time at repeat compared to novel images (Fig. 1B), indicating recognition of previously seen images. We predicted that when monkeys identified a lure image, they would look longer at the lure relative to a repeat image, as the newness of the lure should increase the looking time of a portion of images through dishabituation[16]. Indeed, animals looked significantly longer at lure compared to repeat images (Fig. 1B). Monkeys continued to be engaged in the task across each session, as looking times for lure and repeat images remained consistent throughout (Fig. S2a). Because the number of intervening images between each lure and repeat pair (0-3 images) did not show an effect on looking time performance ($p>0.6$, multi-level ANOVA, Fig. S2B-C), all trial types were pooled regardless of number of intervening images.

**Behavioral Trial classification:** In order to categorize correctly-identified repeat and lure images using monkeys' behavior, we used signal detection theory to compare the effectiveness of two different methods of trial classification: a classic looking time analysis and a newly developed *looking pattern assay*. We defined four categories of response for these analyses. Correctly classified repeat images, where the monkey recognizes the repeat as a previously seen novel image, are called **"repeat"|repeats** (as if the monkey responded "repeat" when shown a repeat), while correctly classified lure images, where the monkey identifies the lure as different than its previously seen novel partner image, are called **"lure"|lures** (Fig. 1C). **"lure"|repeats** are repeats that are incorrectly classified as lures, and **"repeat"|lures** are lures incorrectly classified as repeats.

For the looking time analysis, we identified the amount of time the animal's eye gaze stayed within the bounds of the visual image[15,16]. This analysis, detailed in Figure 1C, achieved a hit rate of 0.39±0.01 and a false alarm rate of 0.34±0.01, which yielded signal detection at $d'=0.14$ (Fig. 1D). This rate indicates that only 39% of lure images would be classified for inclusion in our neural analyses.

In an attempt to improve on this classification rate, we developed a novel *looking pattern assay*, designed to assess monkeys' ability to identify images based on the fixation points of their eyes as they viewed images (Methods) and inspired by methods used to calculate attention maps in humans[17]. Briefly, we identified points on the screen where monkeys fixated on images[18], created attention maps by filling

each of these fixation points with Gaussian kernels and identified the similarity between eye patterns of any pair of images by correlating the kernel fills between the images (Fig. S3). This correlation in the looking pattern assay yields a single value to assess behavior: **ρ**. If monkeys are shown any two random images, the pattern of eye fixations should only coincidentally overlap, and therefore this assay tends towards a low **ρ** value. However, if a novel and repeat image are compared, this assay should tend towards higher values of **ρ** as monkeys identify and attend to features in the previously seen image from memory[19,20] and therefore are more likely to scan the same path[21,22]. So when monkeys are shown a novel and then lure image, if the monkey successfully discriminates the lure (a "lure"|lure), we expect the **ρ** to be relatively low compared to when the monkey misclassifies the lure image as a repeat (a "repeat"|lure). In this same sense, when monkeys are shown a novel and then repeat image, if the monkey successfully discriminates the repeat (a "repeat|repeat), we expect the **ρ** to be relatively high compared to when the monkey fails to identify the repeat (a "lure"|repeat). We can then set a single threshold for **ρ** to classify lures and repeats with this logic for both of these scenarios (Fig. 1C). Using the best threshold for separating "lure"|lures from "repeat"|lures for each individual session (Methods), the looking pattern assay achieved a "lure"|lure rate of 0.62±0.02 compared to a "lure"|repeat rate of 0.40±0.02 (Fig. 1D). This yields a d' of 0.64, a 4.6x improvement over preferential looking, while also achieving this classification level with a higher proportion of trials (i.e., 62% of lures were identified as "lure"|lures compared to 39% for preferential looking, Fig. 1D). The looking pattern assay was also a marked improvement (1.6x) on classification of trials by selecting "lure"|lure and "lure"|repeat images as those lures and repeats with >1 fixation point (d'=0.4, Fig. 1D), indicating that the looking pattern assay utilizes information from the scanpaths[21,22] and is not just an artifact of center-bias (Methods). Based on these findings, we behaviorally defined pattern separation as trials where the monkey successfully discriminated lure images from novel images using our looking pattern assay ("lure"|lures), and behaviorally defined recognition as trials where the monkey successfully recognized repeat images ("repeat"|repeats).

**Neurophysiology:** We recorded from 186 single units in the CA3/DG region of the hippocampus in the same three monkeys used in our behavioral analysis during 118 sessions (unit breakdown: rhesus BY=67, rhesus I=112, bonnet B=7). Responses across these neurons during image presentation were highly variable (mean firing rate for 161 neurons < 20 Hz. = 4.8±4.0 Hz.; for 25 putative interneurons ≥ 20 Hz.[23] = 34.8±12.5 Hz.) with a population sparseness ($a^p$=0.37, Methods) similar to previous recordings in monkey CA3 ($a^p$=0.33 [24]). These neurons were recorded throughout the anterior two-thirds of the hippocampus (Fig. S4-5). Estimates of recording locations within each hippocampal subfield were performed by comparing labels in a rhesus macaque brain atlas[25] to MRI for rhesus BY and bonnet B and a combination of MRI (Fig. S4) and histology (Fig. S5) for rhesus I.

**Population analysis:** We first performed a population analysis to get an overall sense of how our pooled neurons respond during pattern separation and

recognition in the hippocampus. We aimed to address our first hypothesis, that CA3/DG neurons would treat lure images more like novel images than repeat images, and therefore maintain similar firing rates between novel and lure images when animals succeed in behavioral pattern separation, but respond differentially to novel and repeat images during successful recognition. We found the average firing rate of each neuron during the fixation periods at the beginning of each trial as well as during the presentation of novel, "lure"|lure (our pattern separation condition), and "repeat"|repeat (our recognition condition) images. There was no evidence of the firing rates during any of these periods coming from different distributions (p=0.85, multi-level ANOVA after log transformation, Methods). Therefore, we required more specific analyses to investigate if hippocampal neurons respond differently during pattern separation and recognition.

First, we asked if we could identify a difference in hippocampal responses between these two key behaviors by analyzing the distribution of firing rates for each pooled trial type. If we assume our population of 186 neurons is a reasonable sample of the active neurons throughout the hippocampus, and that any given trial in any given session is on equal footing, we can combine all trials across all neurons into very large pools of trials split by trial type (total trials recorded from each trial type: 27614 novel, 9671 lure and 9178 repeat trials). Pooling trials in this manner—after normalizing each to their baseline firing rate—is akin to visualizing how 27614 hippocampal neurons would simultaneously respond to a *single* novel trial, 9671 neurons to a single lure trial or 9178 neurons to a single repeat trial.

A histogram of the distribution of firing rates created by normalizing trial counts to give equal proportions of each trial type is shown in Fig. 2A. The three distributions are significantly different (p=1.4E-6, multi-level ANOVA of log-transformed z-scores, Methods). Notably, lures show a proportional increase in trials with positive z-score firing rates compared to repeats (note the increase in the red bars compared to the blue bars from 1 to 4), while the repeat distribution shows a proportional increase in negative z-score firing rates compared to lures (note the increase in the blue bar compared to the red bar from -3 to -1).

To better visualize how the population firing rates are distributed amongst each group of trials, we created quantile-quantile (QQ) plots of the firing rate counts for both lure v. novel and repeat v. novel trials (Fig. 2B)[26]. QQ-plots provide a way to compare how two sets of data are distributed, with a deviation from the line at y=x in a given range representing a difference in the proportion of one distribution over the other within that range. Comparing lure firing rates with novel firing rates, the QQ-plot shows little deviation between the populations as the line hugs y=x until novel firing rates exceed a z-score of 3 (Fig. 2B, red). Indeed, the lure and novel QQ distributions do not show a significant difference (Fig. 2B). However, repeat firing rates show a relatively larger difference from novel firing rates, as the proportion of firing rates begins to drop above a z-score of 1 and continues to decline as the firing rates get larger (Fig. 2B, blue). This pattern is confirmed statistically, as the novel and repeat QQ distributions are significantly different, and notably, the lure and

196 repeat QQ distributions also show a significant difference (Fig. 2B). These same
197 trends are also significant when we classify trials using our behavioral metrics (Fig.
198 S6). In sum, this pattern of firing is in line with our hypothesis that neurons
199 maintain a relatively similar distribution of firing rates when animals behaviorally
200 perform pattern separation of novel and lure images, but show a relatively
201 dissimilar distribution of firing rates when animals behaviorally recognize repeats.

202 **Single cell analyses:** Next, we ask if the pattern of firing rates shown during pattern
203 separation in our population analysis can be seen at the level of individual neurons.
204 In our task, in line with our overarching hypothesis, we expect a given hippocampal
205 neuron participating in pattern separation to show small changes in firing rate
206 between novel and lure images and therefore respond at similar rates to these two
207 trial types. However, if the animal recognizes a previously seen image, we expect the
208 neuron to show larger changes in firing rate between novel and repeat images and
209 therefore less similar responses.

210 To test our hypothesis for each neuron, we used the behavioral results from our
211 looking pattern assay to classify separate pools of "lure"|lure and "repeat"|repeat
212 trials for each session. For this particular analysis, we used a single (stricter)
213 threshold to classify trials instead of a different threshold for each session, which
214 allowed us to more selectively classify "repeat"|repeat trials without sacrificing
215 selectivity for "lure"|lure trials (Fig. S7 and Methods). We found the correlation
216 between the vectors of firing rates between the pool of "lure"|lure trials and their
217 respective novel trial vector, as well as between the vector of firing rates for the
218 pool of "repeat"|repeat trials and their respective novel trial vector, to assess the
219 similarity in firing responses to these trial types for each separate neuron (Fig. 3A).
220 We kept only the 137/186 neurons recorded during at least 10 "lure"|lure and 10
221 "repeat"|repeat trials and assessed the significance of the 137 "lure"|lure and 137
222 "repeat"|repeat correlations using resampling (Methods).

223 We found 35/137 (26%) of CA3/DG neurons had significant correlations between
224 "lure"|lure and novel trials (Fig. 3B, pink) but not "repeat"|repeat and novel trials. In
225 contrast, only 13/137 (9%) of neurons had significant correlations between
226 "repeat"|repeat and novel trials but not "lure"|lure and novel trials (Fig. 3B, cyan).
227 This relatively larger proportion of neurons with significant correlations for
228 "lure"|lure than for "repeat"|repeat is not expected by chance ($p=4.7E-4$, $\chi^2$
229 (12.2,1)). We found a similar trend when performing the same analysis using all
230 trials (i.e. all lures and repeats without behavioral classification) or our standard
231 method of classifying trial types using different thresholds for each session (Fig. S8).
232 Therefore, CA3/DG neurons are more likely to maintain similar levels of firing rate
233 during "lure"|lure than "repeat"|repeat trials, supporting our hypothesis that
234 neurons in this region express pattern separation by responding to lure images with
235 similar firing levels as novel images.

236 In the previous analysis, we used the results of our looking pattern assay to select
237 for pools of trials during successful pattern separation ("lure"|lure) and successful
238 recognition ("repeat"|repeat). However, we can perform an even more detailed

239 analysis by using the behavioral output from our assay (**ρ**) for each single
240 comparison (e.g. novel v. "lure"|lure) and plotting it vs. the change in firing rate
241 (ΔFR) of a given neuron between each image presentation (Figure 4A). On these
242 graphs, in line with our hypothesis that hippocampal neurons show similar firing
243 levels to lure images as novel images during successful pattern separation, we
244 anticipate that when monkeys succeed in pattern separation of lure images (low **ρ**)
245 neurons will show only a small ΔFR between lure and novel images. However, when
246 monkeys show relatively poor behavioral evidence of pattern separation of lure
247 images (high **ρ**), we expect neural ΔFRs to be larger. Therefore, positive correlations
248 on these plots for "lure"|lure trials are evidence for our hypothesis: that CA3/DG
249 neurons maintain more similar levels of firing during successful pattern separation.

250 We found the correlation, R, between ΔFR and **ρ** (as in Fig. 4A) for "lure"|lure trials
251 for each of the 76 neurons with at least 20 "lure"|lure and 20 "lure"|repeat trials and
252 a minimum FR of 0.5 Hz (more strict selection criteria were used due to the sample
253 size needed to form each plot as in Fig. 4A). The histogram of R values for these
254 neurons shows a significantly positive skew—as compared to the null expectation of
255 a population centered at zero—for the "lure"|lure trials (Fig. 4B, red; "lure"|lures,
256 median=0.15, p=1.2E-4, sign test). We then compared these values to a similar
257 histogram of R values for the "lure"|repeats (Fig. 4B, blue), which are when monkeys
258 incorrectly classified a repeat as a lure, an indication that the animal did not form a
259 strong memory of the novel image and then failed to recognize the repeat image. In
260 this case, neurons should respond more like they were shown random pairs of novel
261 images, which would make the relationship between ΔFR and **ρ** less correlated and
262 therefore R smaller. This comparison acts as a control, since if R values are similar
263 for "lure"|repeats as for "lure"|lures, our hypothesized signature of pattern
264 separation would be no better on misclassified repeats as correctly classified lures.
265 Indeed, for these same 76 neurons the R values for "lure"|repeats were significantly
266 lower than "lure"|lures (p=0.0043, multi-level ANOVA (Methods)). These data
267 indicate that when monkeys successfully identify a lure image, which we consider
268 successful pattern separation, CA3/DG hippocampal neurons are more likely to fire
269 at rates akin to when they view novel images.

270 Next, we asked if this pattern separation signal seen across the population of
271 CA3/DG neurons is driven by a small subset of "pattern separating" neurons. We
272 took these 76 neurons and removed the 16 neurons with significant ($p<0.05$) R
273 values (Fig. S9). We reasoned if pattern separation was being driven by a subset of
274 neurons, by removing the group of neurons with significant signals we would no
275 longer see the positive skew towards pattern separation across the population as
276 shown in Figs. 4B-C. Crucially, the histogram of R values for the remaining 60
277 neurons still shows a significantly positive skew for "lure"|lures (Fig. 4D;
278 median=0.11, p=0.027, sign test). This analysis indicates that the neural bias
279 towards pattern separation in Fig. 4B-C does not appear to be driven by a small
280 subset of neurons, but instead by a large proportion of CA3/DG neurons that
281 contribute with varying degrees to pattern separation.

Finally, we asked if the CA3/DG area of the hippocampus shows stronger signals for pattern separation or recognition memory by comparing the populations of neurons tuned to each process. Neural evidence for recognition memory has previously been shown in the monkey hippocampus by correlating the absolute change in firing rate (ΔFR) between novel and repeat images with the change in looking times[15]. To emulate this analysis (c.f. Figure 4D in reference [15]), we created graphs of ΔFR v. change in looking time for the 148 CA3/DG neurons that were recorded during the presentation of at least 30 repeat trials with a minimum firing rate of 0.5 Hz. The expectation is that when there is evidence that animals better recognize repeat images, indicated by larger decreases in looking time compared to novel images, their neural ΔFRs will increase. Correlations between ΔFR and looking times (R') show a significant trend towards recognition memory across the neural population (median=0.046, p=0.004, sign test; Fig. 4C). However, comparing the 76 R values for "lure"|lures—indicative of pattern separation—vs. the 148 R' values for repeats—indicative of recognition—shows the distribution of R values is significantly larger (Fig. 4C, p=4.7E-4, multi-level ANOVA). Further, only 6/148 neurons show a significant R' value ($p<0.05$), which is significantly less than the 16/76 neurons with significant R values to "lure"|lures (p=5.2E-5, $\chi^2$ (16.4,1)). In sum, CA3/DG hippocampal neurons are more likely to show firing patterns indicative of pattern separation than recognition memory.

**Discussion:**

We recorded from single neurons in the monkey hippocampus as animals serially viewed novel, similar (lure) and repeat images. We show that when there is evidence that monkeys succeeded in behavioral pattern separation by identifying a lure image as distinct from a recently seen novel image, single CA3/DG hippocampal neurons treat the lure more like a novel image than a repeat image, and therefore maintain similar firing rates between the lure and novel image (Figs. 3&4). On the other hand, when there is evidence that monkeys recognize the repeated presentation of a recently seen novel image, hippocampal neurons show relatively larger changes in firing rate between the novel and repeat image (Figs. 3&4). This pattern of firing is also true at the population level, as the distribution of firing rates when combining trials across neurons shows more similar firing between novel and lure images than between novel and repeat images (Fig. 2). We also find that CA3/DG neurons show evidence of this firing pattern to varying degrees, with a large proportion of the cell population showing evidence of pattern separation (Fig. 4B-D) even though only a small proportion of neurons contribute on any given trial. Finally, we show that CA3/DG neurons are tuned more strongly for pattern separation than recognition memory signals (Fig 4C). These findings confirm predictions from human fMRI studies using a similar task[3] and provide new insight into how individual neurons in CA3/DG respond as a population to achieve pattern separation on a trial-by-trial basis. We discuss the implications for these insights for the code underlying pattern separation below.

Our initial hypothesis, that during successful pattern separation CA3/DG neurons would treat lure images more like the presentation of novel stimuli than repeats, directly follows from BOLD activity patterns measured in the CA3/DG region of the hippocampus in contrast to the surrounding medial temporal lobe[3,4,6]. However, this pattern of firing was not readily apparent when looking at single pairs of trials for a given neuron, but instead was only evident when visualized across many pairs of trials for each neuron (Figs. 3&4) or by pooling trials across our entire CA3/DG population (Fig. 2). To visualize pattern separation at the population level, we combined all lure trials across all neurons into a single pool of 9671 trials, which we consider a reasonable approximation of how 9671 neurons would respond to a single pattern separation event if recorded simultaneously. This analysis might also be analogous to the global signal seen across thousands of neurons in BOLD fMRI of CA3/DG during pattern separation. And, in line with our primary hypothesis, as predicted from fMRI work, the pooled trials of CA3/DG neurons respond to lure images more like novel images than repeat images (Fig. 2). This effect was only clear at the tail end of the firing rate distribution, where only ~8% of lure and ~7% of repeat trials contribute to the range (firing rate≥2) with a clear difference in the distributions (Fig. 2B). The small proportion of trials showing this difference between lure and repeat trials suggests that only a small proportion of neurons participate in a given pattern separation or recognition event, evidence that the pattern separation signal seen with fMRI might be driven by a subpopulation of neurons in this region[27]. This finding also aligns with theoretical work that predicts the necessity for sparse representations to achieve pattern separation in the CA3/DG region of the hippocampus[28], with only a small proportion of neurons contributing to a given pattern separation event (n.b. that while only ~8% of lure trials deviate from the repeat distribution, 71% of neurons contribute to these trials).

While some neurons contribute to pattern separation more than others in our recorded population (i.e., only the 16/76 cells in Fig. S9 and the 35/137 cells in Fig. 3B show statistically significant evidence of pattern separation), we found that a large proportion of these CA3/DG neurons contribute on at least some trials (in principle, each neuron above a correlation of 0 for "lure"|lure in Fig. 4b). In fact, when we remove neurons with significant evidence of pattern separation (Fig. S9), the remaining population is still significantly biased towards our hypothesized pattern separation signal (Fig. 4D). Yet, even for neurons showing statistically significant evidence of this pattern separation signal (e.g. Fig. 4A), there is a large variability in ΔFR, further evidence that neurons do not contribute to pattern separation on most trials but instead are only involved in a limited proportion of pattern separation events. Taken together, these findings in which a large number of neurons contribute to pattern separation, but each neuron only contributes during a small proportion of trials, is evidence of pattern separation being achieved via a sparse distributed coding scheme[24]. Evidence for sparse distributed coding, in which memories are encoded by a small proportion of neurons that each contribute to a small number of memories, has been shown during an episodic memory task in the human hippocampus[26] as well as during spatial exploration in primate

hippocampus[24]. Our results support the idea that hippocampal neurons utilize such a code for pattern separation of images, in which newly presented images are discriminated from recently seen images stored in memory. Studies using multicellular recording from dual regions would be essential to directly[11] show that such *behavioral* pattern separation is achieved via *computational* pattern separation, likely via mossy fibers from the entorhinal cortex to the dentage gyrus granule cells. Such work would also elucidate how the underlying sparse distributed code achieves these computations without relying on pseudopopulations recorded across days.

The population analysis in Fig. 2, where we created a very large pool of trials by combining all trials across all neurons, is inspired by an analysis of human hippocampal neurons where epileptic subjects were tested to recognize single presentations of recently shown words[26]. In this study, a small percentage (1.6%) of recognition trials showed significantly higher spike counts than expected for a typical distribution, which shows on the Q-Q plot as a tail rising from the y=x line. We did not see such a signal in our Q-Q plot for repeat trials, but on the contrary found firing rates tended to drop for repeat trials compared to novel and lure trials. This difference could very well be task-dependent, as subjects in Wixted *et al* were explicitly tasked to recognize well-known words during a retrieval phase after being instructed to study them during an encoding phase. In our task, while monkeys are familiar with the task structure after many sessions of practice before recording, the encoding phase was incidental and the animals only implicitly recognized repeat images. In addition, monkeys were also shown lure images intermixed with repeats, unlike in Wixted *et al*, possibly inciting additional hippocampal pathways other than recognition memory (including pattern separation mechanisms).

Correlates of recognition memory have been shown in the human hippocampus using both fMRI[29,30] and electrophysiological recordings[31-34]. However, short-term recognition in human studies is difficult to disambiguate from long-term memory recall of known objects[35]. Jutras & Buffalo (2010) identified recognition memory signals in the monkey hippocampus using a task similar to ours but without the use of lure images. Their task also involved showing monkeys series of images and they assessed memory performance of repeat images via animal looking times. They found that a population of hippocampal neurons had a larger absolute change in firing rate between novel and repeat images the better the monkey recognized the repeat image. This general phenomenon, where repeat images show either a rise or fall in firing rate compared to the novel image, has also been shown in subpopulations of hippocampal cells from human recordings of epileptic patients tasked to recognize images[7,33,34]. Across our population of neurons we found a significant trend towards this neural correlate of recognition memory (Fig. 4B-C), although neurons were significantly more tuned to pattern separation (Fig. 4C). The relatively weak recognition signal could be due to the fact that our recordings were specifically targeted to CA3/DG regions of hippocampus while recognition signals are typically associated with other hippocampal subregions such as subiculum[15] or CA1[36,37]. Alternatively, the addition of lure images in addition to repeat images in

413 this task—as opposed to only repeat images in Jutras & Buffalo—is likely to alter the
414 hippocampal responses to repeat images, since animals (and their visual pattern
415 separation system) might divert attention to identifying lure images.

416 A number of studies have shown evidence of population codes of spatial pattern
417 separation in the CA3 and dentate gyrus regions of rodent hippocampus[8-12]. These
418 studies report ensembles of CA3 neurons that show evidence of pattern separation
419 or pattern completion dependent on task demands[8], while DG displays more abrupt
420 changes in the population coherence with small changes in context[9,11]. While our
421 results confirm that pattern separation manifests as a population response across a
422 mixture[38] of CA3/DG neurons[9,11], our findings are difficult to compare with these
423 key rodent pattern separation studies. Other than the usual difficulty in comparing
424 behavior across species, pattern separation tasks used in rodents typically involve
425 discrimination of physical environments—with recordings focused on place fields—
426 over the course of minutes. Since the use of monkeys allows us to emulate visual
427 pattern separation tasks used in human fMRI work, we expect our results to be
428 more related to the human work due to task similarity. Future studies can work to
429 bridge these gaps between research models with new task design in rodents
430 (including non-spatial tasks that drive hippocampal responses[39]) and more
431 powerful recording techniques in nonhuman primates and humans.

432 Notably, our use of the looking pattern assay, which assesses pattern separation via
433 the pattern of animal eye fixations, provided a significant step forward in
434 quantifying behavior on a trial-by-trial basis. In particular, we showed that
435 analyzing the patterns of eye fixations with this assay did a better job classifying
436 pattern separation and recognition behavior than standard preferential looking
437 methods (Fig. 1D). Not only can this technique be applied to more advanced
438 memory tasks in monkeys, particularly with more ecological stimuli like videos, but
439 could also be used to implicitly measure pattern separation in humans. For example,
440 this new analysis may be particularly relevant for pattern separation tasks in
441 humans in which markedly different fMRI results have been found when subjects'
442 memory is overtly tested (respond "new"/"old"/"similar")[5] vs. being incidentally
443 probed (respond "indoor"/"outdoor" object)[3,6] (see discussion in Lacy *et al* (2010)).
444 The looking pattern assay might provide an improvement in data collection for
445 these and other human tasks by quantifying pattern separation and recognition
446 behavior without the need for explicit responses.

447 This study identifies how CA3/DG hippocampal neurons respond as monkeys
448 achieve pattern separation of images from those in short term memory. Our single
449 neuron results are consistent with both the pattern of responses shown in human
450 fMRI studies of pattern separation and the population coding of pattern separation
451 via CA3/DG ensembles shown in rodent studies of pattern separation. Further, our
452 data indicate that pattern separation is achieved via a sparse distributed code from
453 across the population of neurons in the hippocampus, with only a small proportion
454 of hippocampal neurons responding on any given pattern separation event despite a
455 large proportion of the population participating in pattern separation overall. With

this sparse distributed code in mind, future studies using large-scale, multicellular recordings will be essential to understand how pattern separation emerges from the combined network effects of a simultaneously recorded population.

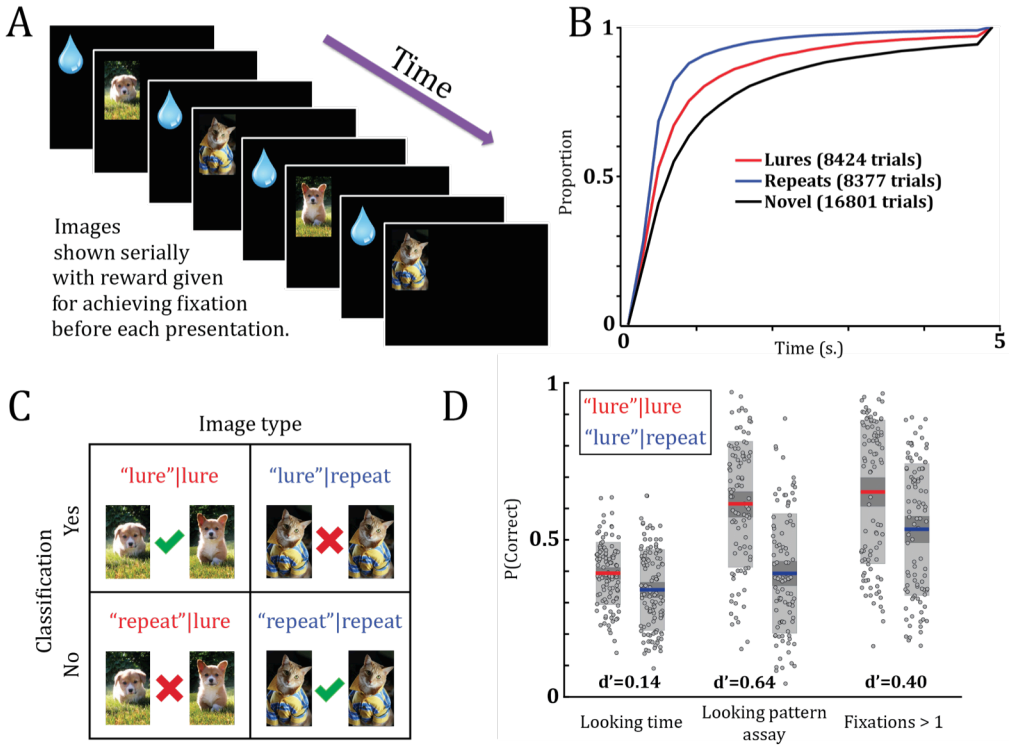


**Figure 1. Task outline and behavioral results. A)** Diagram of task structure. In this example, the monkey would see two novel (never-before-seen) images followed by a lure image (3rd image) and then a repeat image (4th image). Images are centered on the screen. Reward is given before every image presentation when fixation to a center dot is achieved. **B)** Cumulative histogram of looking times pooled across all animals and separated by trial type. Monkeys looked significantly longer at novel compared to repeat images (novel mean=1.40 s. v. repeat mean=0.73 s., p=9.6E-10) and lure compared to repeat images (lure mean=1.04 s. v. repeat mean=0.73 s., p=2.0E-8). Monkeys also looked longer at novel compared to lure images (p=1.1E-8) (Tukey's HSD of group means after multi-level ANOVA for all pairwise comparisons, Methods), as expected since animals only likely discriminate a proportion of lure images. **C)** Chart of the behavioral classification scheme inspired by signal detection theory. Image type indicates if a lure or repeat was shown to the monkey, while classification indicates how the monkey treated the image based on the behavioral metric. For the looking time analysis, when monkeys looked at a repeat image for shorter than its respective novel image, this was considered a "repeat"|repeat. When monkeys looked at a lure image longer than its respective novel image, we considered it a "lure"|lure. For the looking pattern assay, when **ρ** between a repeat and novel image was higher than threshold, this was considered a "repeat"|repeat. And when **ρ** between a lure and novel image was lower than threshold, we considered this a "lure"|lure. Therefore, when **ρ** is lower than threshold on

repeats—a false alarm event—we call this a “lure”|repeat. And when **ρ** is higher than threshold on lures—a false negative event—we call this a “repeat”|lure. **D)** Hit rate (a hit being a “lure”|lure) and false alarm rate (a false alarm being a “lure”|repeat) for 88 sessions in 3 monkeys for three classification methods (Methods). Left: looking time assay. Center: looking pattern assay using the best **ρ** threshold value for each session. Right: classification of hits and false alarms using only lures and repeats with >1 fixation. Each classification method was done with the same threshold for both “lure”|lure v. “repeat”|lure and “lure”|repeat v. “repeat”|repeat comparisons, making the d’ values an unbiased assessment of behavioral classification. Averages are shown by colored lines, shaded boxes are the 95% confidence interval (dark gray) and the standard deviation (light gray).

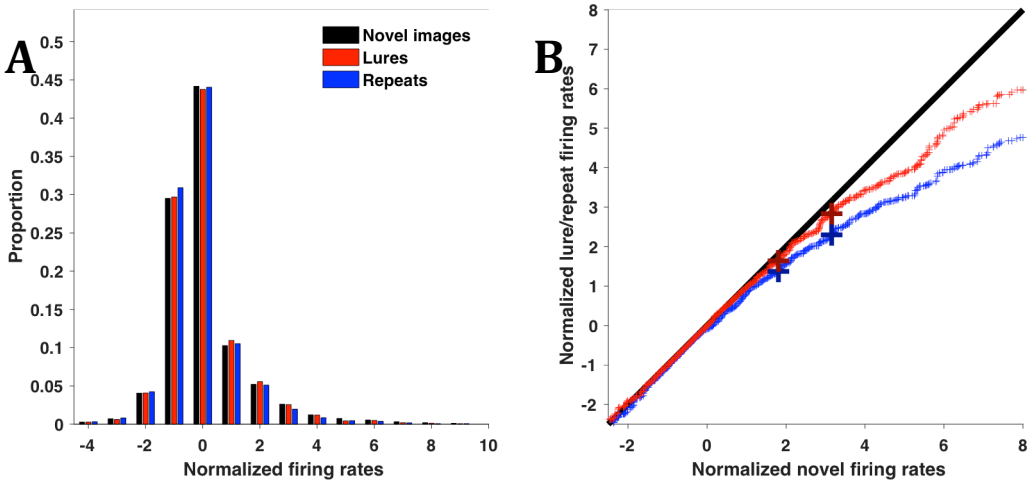


**Figure 2. Population analysis of firing rates across neurons. A)** Histogram of normalized firing rates (z-score) for all novel, lure and repeat trials pooled across neurons. That is, 27614 trials with accumulated spikes during novel image presentation, 9671 during lure presentation and 9178 during repeat presentation. Only trials where the animal viewed the image for at least 400 ms were included in these pools so we could accumulate spikes over the period 200-500 ms after image presentation (after [26]). These firing rates were then normalized separately for each neuron by z-scoring based on the average and standard deviation of the fixation period firing rates for that neuron. **B)** Quantile-quantile (QQ) plot of novel v. lure trials (red) and novel v. repeat trials (blue). Black line is y=x, which would represent populations with equal firing rate distributions. After confirming that these three firing rate distributions are not likely to come from a single distribution of firing rates (p=1.4E-6, multi-level ANOVA), we can assess the statistical significance of pairwise QQ comparisons using a two-sample Kolmogorov-Smirnov test (Methods). The novel and lure trials do not show evidence of coming from different distributions (p=0.37). However, both the comparison between the novel and repeat trials (p=5.2E-5) as well as the comparison between the lure and repeat trials (p=4.8E-3) show significant evidence of coming from two different distributions (Bonferroni-corrected alpha = 0.017). The large crosses indicate the point at which 90 (left) and 95% (right) of lure (maroon) and repeat (dark blue) trials are below that normalized firing rate. Note that the repeat trial QQ distribution only begins to deviate from the lure trial QQ distribution at the 90% quantile near a normalized firing rate of 2. Only 8.3% (806/9671) of lure trials reach this firing rate, although 71% of neurons contribute to these 806 trials (mean±std = 3.9±6.7 trials/neuron). In comparison, the lure trial QQ distribution only begins to deviate from the novel distribution (y=x) at the 95% quantile near a normalized firing rate of 3. Similar results were seen when we limited our sample size to only trials classified as "lure"|lures and "repeat"|repeats (Fig. S6).

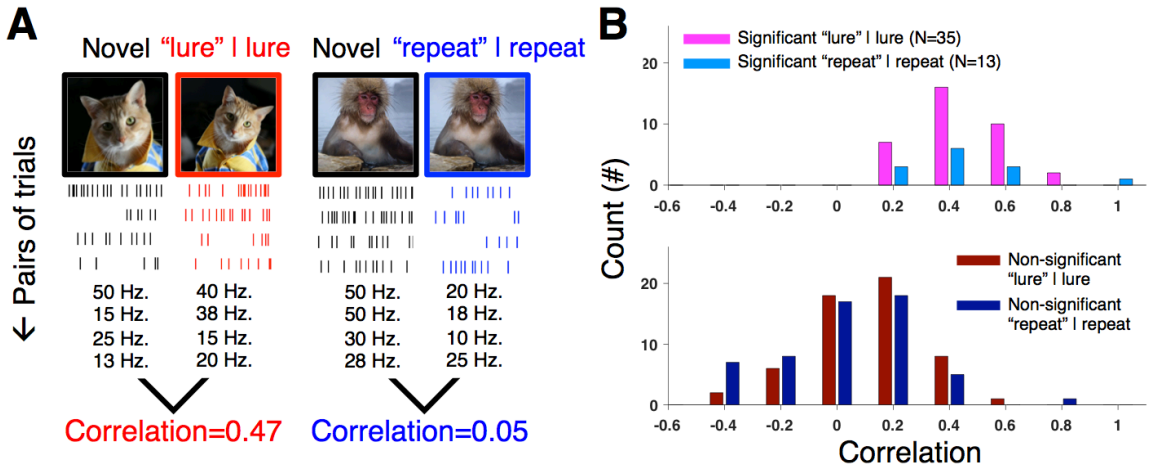


**Figure 3. Correlated firing rates of single cells between trial types. A)** Diagram showing how population firing rate correlations are calculated. Note that for each row the pair of images—novel v. "lure"|lure and novel v. "repeat"|repeat—were always different, as novel and lure images were never shown to the monkey more than once (and repeats not more than twice). (Left) Raster plots of the novel and matching "lure"|lure trials for a single neuron are converted to two vectors of firing rates. For the "lure"|lure pool, we found the firing rate from a given neuron during each lure image presentation and created a vector of these firing rates. We then took the novel image pairs that were shown before each of these lure images and created a separate vector of firing rates. The "lure"|lure and novel image vectors could then be correlated to measure the similarity in firing between them. The first 4 elements in the "lure"|lure comparisons are shown for an example neuron. We then measured the correlation between these vectors (correlation=0.47 in this test example for 4 rows of trials) separately for each neuron in our population. (Right) The same process was also done to find the similarity in firing for each neuron between "repeat"|repeat and the novel image pairs that were shown before each of these repeat images. Correlation values were also found between "repeat"|repeats and their respective novel images for each neuron (correlation=0.05 in this example). For simplicity only 0.4 s. of each trial is shown, but in the real task image presentation times were variable as they were under control of the monkey. **B)** Breakdown of significant neurons determined by resampling method. Neurons with significant correlation values only for "lure"|lures (N=35, pink) and "repeat"|repeats (N=13, light blue) are shown on the top, while neurons with nonsignificant correlation values for both "lure"|lures and "repeat"|repeats are shown on the bottom. Resampling is a practical way to account for neural firing rates with a wide range of firing rate variability and sparseness as typically shown in the hippocampus[26,28,40]. Here the surrogate data models the firing distribution for each individual neuron to account for this sparse firing[41].

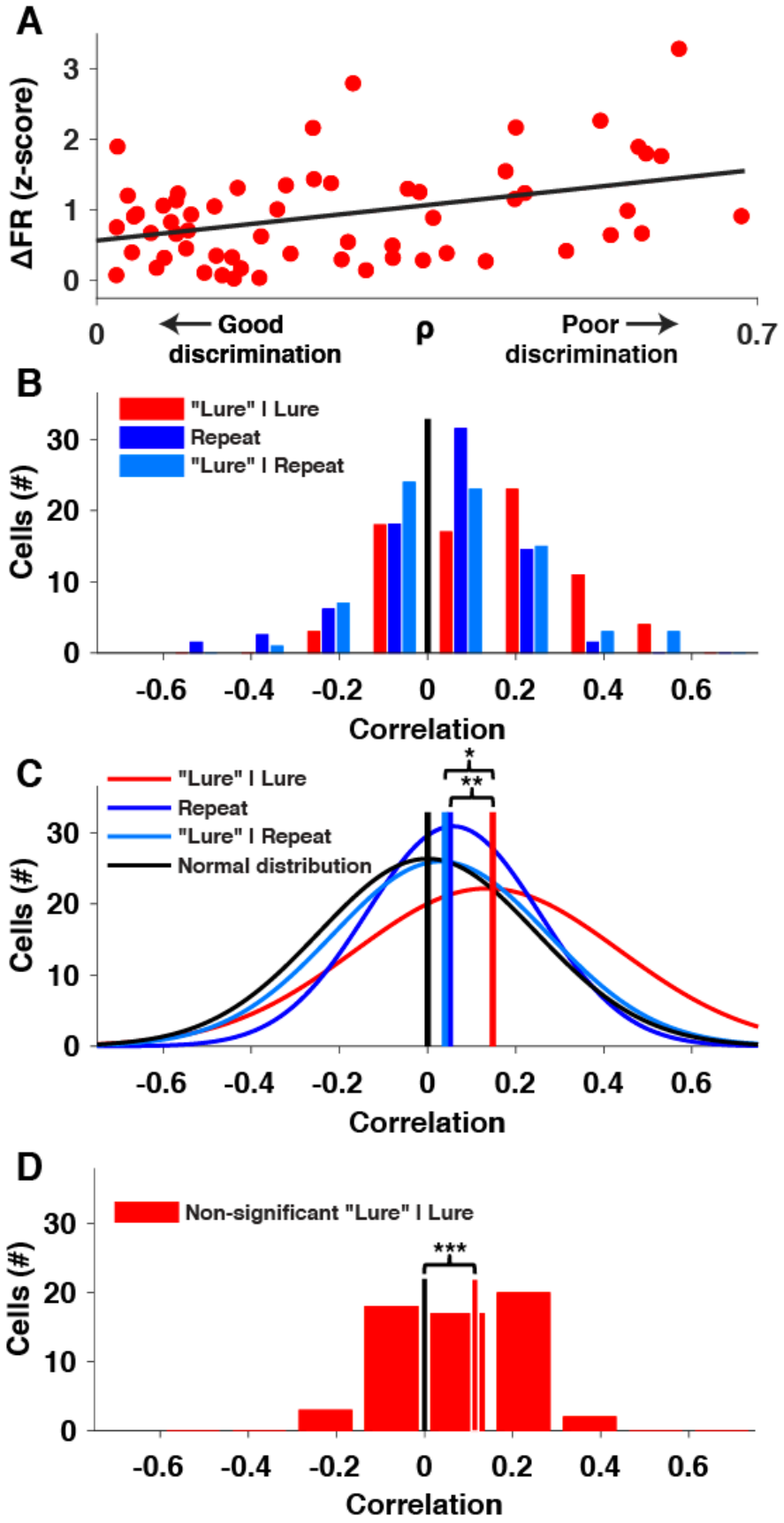
A
ΔFR (z-score)
3
2
1
0
0
Good discrimination
ρ
Poor discrimination
0.7
B
"Lure" I Lure
Repeat
"Lure" I Repeat
Cells (#)
30
20
10
0
-0.6
-0.4
-0.2
0
0.2
0.4
0.6
Correlation
C
"Lure" I Lure
Repeat
"Lure" I Repeat
Normal distribution
*
**
Cells (#)
30
20
10
0
-0.6
-0.4
-0.2
0
0.2
0.4
0.6
Correlation
D
Non-significant "Lure" I Lure
***
Cells (#)
30
20
10
0
-0.6
-0.4
-0.2
0
0.2
0.4
0.6
Correlation

555

**Figure 4. Neural firing rates correspond to behavioral pattern separation for single cells. A)** Scatterplot for an example neuron, where each point shows the change in firing rate (ΔFR) v. the looking pattern assay value **ρ** for a single novel and "lure"|lure image pair. Black line is a linear fit of the points, which have a correlation of R=0.43 (p=3.3e-4, Pearson). Positive R values indicate more similar firing rates (smaller ΔFR) during better behavioral pattern separation (smaller **ρ**). For this analysis, we took each neuron and found ΔFR between each "lure"|lure and its paired novel image by aggregating spike counts during the presentation of each image, dividing by the time the monkey looked at that image, z-scoring using the fixation period firing rate for that neuron, and finding the absolute difference in rate between the pair ( $\Delta FR = |z(novel_FR) - z(lure_FR)|$ , Methods). Since the strength of the correlations between neural firing rates and behavior depend on the number of points populating each scatterplot, we limited this analysis to the 76 single units that were recorded for at least 20 "lure"|lure trials, 20 "lure"|repeat trials and had an average firing rate of at least 0.5 Hz. during all image presentations. **B)** Histogram of the correlation values (R) between ΔFR and **ρ** for "lure"|lure (red) and "lure"|repeat (light blue) for these 76 neurons. Repeat (blue) shows correlations (R') between ΔFR and the change in looking time (after [15]) between novel v. repeat images for 158 neurons with at least 20 repeat trials; this histogram is normalized by neuron count to match the numbers for "lure"|lure and "lure"|repeat. Positive R' values indicate larger changes in firing rate for better recognition memory. Black line is at x=0 for visual effect. **C)** Gaussian fits of each set of data in **B**, along with a null Gaussian distribution (black) for visual comparison centered at 0 with σ averaged from the 3 datasets. The vertical lines indicate the median of each distribution. *"lure"|lure v. "lure"|repeat, p=0.0043; **"lure"|lure v. Repeat, p=4.7E-4 (multi-level ANOVA, Methods). **D)** Same "lure"|lure data as in B, but with the 16/76 neurons with significant correlations removed. Superimposed red line indicates median. ***p=0.027 (sign test).

## Methods

**Subjects:** Two female rhesus macaque (rhesus BY=6.7 kg., age 11; rhesus I=5.7 kg., age 6) and one male bonnet macaque (bonnet B=8.9 kg., age 12) monkey were used for experiments. Animals were surgically implanted with titanium headposts using aseptic techniques under general anesthesia and then trained to be comfortable visually interacting with a computer monitor for juice reward while being headposted during a multiple hour recording session. All procedures and treatments were done in accordance with NIH guidelines and were approved by the New York University Animal Welfare Committee.

**Behavior:** Animals were positioned in a primate testing chair (Crist Instruments) and trained to fixate on a 19-inch LCD monitor (Dell) positioned 0.45 m. from center of screen to left eye. Eye position on screen was monitored by an infrared camera at 240 Hz. resolution (IScan, Inc.) and linearly interpolated to 200 Hz. resolution so each time bin of eye position was 5 ms The task was programmed in Presentation (Neurobehavioral Systems).

**Task:** In our main task, monkeys were shown series of images centered on a computer screen. Each trial began with the presentation of a centered red dot of radius 1°. Animals received 0.35mL juice reward for maintaining fixation within a 1.3° radius around the center of this dot for 500 ms Next, animals fixate on a blue centered dot with the same parameters as the last one and when this 'pre-fixation' is maintained for 300 ms, a centered image is presented on the screen. Animals were allowed to view the image for up to 10 seconds but the image was removed—and the trial completed—when monkeys looked outside the bounds of the image with a 1.85° surrounding buffer (that is, fixation did not break until the position of the eye was outside of the actual image dimensions plus a 1.85° rectangular frame). We kept images at their native resolution unless their longest dimension was >600 pixels (22.2°), in which case the image was scaled down such that the longest dimension was set to this length. Animals were initially trained on a version of the task with only novel and repeat images (identical to the visual preferential looking task [VPLT][15]) with no lure images. This was done because images used during neurophysiology were never used again for another recording session and we wanted to save most of the lure image set for recording sessions. In a few sessions before recording the animal performed the full task to acclimate to the presence of lure images.

Each image was either 1) a novel image, which was never before shown to the monkey 2) a repeat image, which was the repeat of a novel image shown to the monkey 1-4 serial positions after the initial presentation or 3) a lure image, which was an image similar to a novel image shown 1-4 serial positions after initial presentation. Examples of lure images are shown in Fig. S1. On any given trial—except the first—there was a 3/5 chance of seeing a novel trial and a 1/5 chance of seeing either a lure or a repeat of a previously shown novel image. Therefore, 1/5 of novel trials were foil images, which were only shown once and therefore were not

628 followed by a repeat of the foil or a similar lure version. Lure and repeat images
629 were shown within the next 1:4 trials after their associated novel image (0-3
630 intervening images). Lures and repeats both had an equal proportion of these
631 intervening image numbers in each session.

632 We compiled a set of 6450 lure image pairs, 6450 repeat image pairs and 6450 foils.
633 This large set of pictures allowed us to perform all neural recording sessions with
634 images the monkeys had never before seen, thereby ensuring this task would be
635 focused on short term memory encoding and retrieval. Images were hand-picked
636 from a wide variety of sources and are available for research purposes upon
637 request. Images were collected from the following sources: a previous pattern
638 separation study[3], [42] (available at
639 http://www.vision.caltech.edu/savarese/3Ddataset.html), Hemera photo objects
640 25,000 (Hemera, 1999), [43] (available at http://fei.edu.br/~cet/facedatabase.html),
641 [44] (available at http://vision.stanford.edu/lijiali/event_dataset/), [45] (available at
642 http://www.image-net.org/), screenshots from webpages, and screenshots taken
643 from Youtube.com videos and DVDs using custom software in Matlab. This provided
644 a wide array of image types which included objects, environments, faces, people,
645 animals, etc. (Fig. S1). To ensure there were no unintentional repeats or overly
646 similar lure images across our 19,350 images, we used Visipics V1.3
647 (www.visipics.com) to compare images and manually remove those with high
648 similarity.

649 Despite reward being incidental to the behavior in the task, monkeys showed
650 sustained interest in images throughout each session. As shown in Figure S2a, while
651 there was a slight decline in looking time of novel images near the end of the
652 average session, there was no noticeable decline in looking times for lure or repeat
653 images. We also found that monkeys showed no intent to 'cheat' the task by
654 immediately saccadding outside the bounds of the image to get to the next trial, as
655 animals looked at 96.4% of all images for at least 250 ms, and saccadic reaction
656 times in monkeys rarely exceed 200 ms[46]).

657 **Behavioral trial classification:** We assessed behavior for animals during the
658 88/118 sessions where at least 50 lures and repeats were shown to the animals
659 (Rhesus BY=37, Rhesus I=43 and Bonnet B = 8). The remaining sessions showed
660 similar average values for our classification metrics but were excluded for
661 quantification of our assays due to their small sample size (and therefore increased
662 variance).

663 For our first analysis of behavior, we used looking times as a proxy for memory
664 performance. These times were measured as the time from image presentation until
665 the animal looked outside the bounds of the image (including the aforementioned
666 1.85° spatial buffer around each image). To test for differences between these
667 looking times based on trial types, we used multi-level ANOVA to compare looking
668 times of novel, lure and repeat images. Our predictors included categorical variables
669 for the three monkeys and the three trial types tested, with the dependent variable
670 the looking time on each trial. Our goal is to test for differences between trial types

after regressing out the variance of the looking times between monkeys and the interaction of monkeys X trial types. Therefore, the resulting p-value we report indicates only the significance of the trial type factor. We used the anovan function in Matlab to make this comparison and then used the multcompare function to perform pairwise, multiple comparisons—corrected Tukey HSD tests between pairs of trial types.

We used a signal detection theory framework to classify behavior on lure and repeat trials, with the true positive condition indicating the monkey looked longer at a lure image than its previously shown accompanying novel image. We refer to such a trial as a "lure"|lure, as if the monkey responded "lure" to a given lure image. The true negative condition is when the animal looked less at a repeat image than its previously shown accompanying novel image, which we refer to as a "repeat"|repeat. Therefore, false negatives are when a lure was viewed for less time than its accompanying novel image, which we refer to as a "repeat"|lure, and false positives are when a repeat is viewed for more time than its accompanying novel trial, which we refer to as a "lure"|repeat.

As shown in the main text, we achieved better classification performance using a looking pattern assay (Fig. 1D), which used the pattern of eye fixations instead of looking times to compare pairs of trials (i.e. novel v. lure and novel v. repeat). This method is inspired by attention map or visual saliency methods used in humans[17,47]. First, for a given comparison (e.g. a novel image and its paired lure image), we found the fixation points separately for each image. Instead of defining fixation by an arbitrary criterion like a minimum amount of time the fixation remained in one location, we used a k-means—based algorithm which was specifically developed for patterns of fixations from monkeys (ClusterFix http://buffalo-lab.physiol.washington.edu/ClusterFix.html)[18]. We took these fixation points on each image and plotted 2-dimensional Gaussian kernels centered at each point with identical weight for each point. The σ for each Gaussian was set to the standard deviation of the distances from the center of the fixation point of each time bin during fixation. An example is shown in Figure S3, where fixation points from the eyetracking data are shown superimposed over a novel and lure image (top). The Gaussian fill of these kernels is shown on the bottom, which create "attention maps." Finally, the rows of each attention map were appended into two single vectors and the Spearman correlation (**ρ**) between them was calculated. A novel and lure pair (or a novel and repeat pair) without at least 1 fixation on each image were discarded as trial classification for these trials was not possible.

We used this correlation value, **ρ**, to classify trials with a signal detection theory approach similar to what was described for looking times above. If we calculated **ρ** for patterns of eye fixations between two completely unrelated images, which would have two random patterns of eye data (except that they both start in the middle of the screen), we would expect a low **ρ** value. On the other hand, when we show two identical images, we expect the patterns of fixations to be more similar, as animals will be more likely to examine the salient features between the two identical images

714 and yield a higher **ρ** value if they recognize the image as a repeat. This effect of
715 similar eyetraces for repeated stimuli has been shown experimentally in humans
716 [21,22], while there is a notable history showing that looking patterns are related to
717 hippocampally-dependent memory[19,20].

718 Therefore, when the monkey recognizes a repeat image as similar to a previous
719 novel image, a "repeat"|repeat, we expect a relatively high **ρ** value. And when the
720 monkey fails to recognize a repeat image, a "lure"|repeat, we expect a relatively
721 lower **ρ** value. On the other hand, when the monkey treats a lure image as different
722 from a previous novel image, a "lure"|lure, we expect a lower **ρ** value. And when the
723 monkey fails to identify a lure image as different from a novel image but instead
724 treats it more like a repeat, a "repeat"|lure, we expect a higher **ρ** value. By setting a
725 threshold value of **ρ** we can then classify repeats into "repeat"|repeat or
726 "lure"|repeat and lures into "lure"|lure or "repeat"|lure. To find what threshold
727 value optimally classified repeats and lures for each session, we made an ROC curve
728 using "lure"|lure as true positives and "lure"|repeat as false alarms and
729 parametrically tested values of **ρ** to find one that maximized d'. The median 'best
730 threshold' calculated for each session was 0.525 and the mean value was 0.56±0.03
731 (SE). These best thresholds were used for our behavioral analysis in Figure 1D as
732 well as the neural analyses in Figures 4, S6, S8B and S9.

733 We also classified repeat and lure trials by just using a single threshold for all
734 sessions. While using a constant threshold worsened our behavioral classification
735 (session average d'=0.39 as opposed to 0.64 for best threshold, Fig. S7), we used this
736 metric when we wanted to more selectively classify recognition trials
737 ("repeat"|repeat). The intuition for this is that the best threshold calculations
738 described in the previous paragraph maximize the difference between true positives
739 ("lure"|lure) and false alarms ("lure"|repeat). This method left us with 40% of
740 repeat trials selected as "lure"|repeat (Fig. 1D). Therefore, the other 60% of repeat
741 images were classified as "repeat"|repeat. To more discriminatingly select
742 "repeat"|repeat trials, when we set a relatively higher single threshold of 0.6 for all
743 sessions, the average number of repeat trials classified as "repeat"|repeat was
744 reduced to 41% (a refinement of 19%). Meanwhile, setting this constant 0.6 value
745 only came at a cost of classifying lures as "lure"|lure at 70% (8% less refined than
746 best threshold, Fig. 1D). We used a single threshold for Figure 3, since we wanted to
747 compare pattern separation ("lure"|lure) v. recognition ("repeat"|repeat) with this
748 more refined selection of repeat trials. However, we still show similar trends when
749 using the less-selective-for-recognition best threshold method (Fig. S8B).

750 As a control, we created a classification scheme for lure and repeat trials in which
751 we identified the number of fixation points (using ClusterFix, as explained above)
752 for each lure and repeat image and classified lures with >1 fixation point as
753 "lure"|lure and repeats with >1 fixation point as "repeat"|repeat. The rationale for
754 this control is that monkeys are required to begin fixation at the center of each
755 image, so the simplest comparison we can make is between a pair of novel and lure
756 (or novel and repeat) images that each have 1 fixation point in the center before the

757 monkey saccades outside the bounds of each. An argument could be made that our
758 looking pattern assay only achieves positive d' by classifying such trials as
759 "repeat"|repeat or "repeat"|lure while the remaining trials with more rich eyetraces
760 are classified as "lure"|lure or "lure"|repeat. We show that while such a system does
761 show a positive d' value of 0.4, our looking pattern assay improves on this value by
762 60% to 0.64.

763 **Neurophysiology:** Circular HDPE plastic recording chambers (Rogue Research)
764 were custom-fit to the skull of each monkey via structural MRI scans, placed
765 perpendicularly to the horizontal plane in stereotaxic coordinates and dorsally
766 above the anterior 2/3 of the left hippocampus. Single unit recordings were
767 performed by lowering glass-insulated electrodes (~1 MΩ impedance, Alpha
768 Omega) or glass-insulated tetrodes (~0.5 MΩ impedance for all 4 shafts, Thomas
769 Recording, Germany) via an electric (NAN Instruments, Israel) or hydraulic
770 microdrive (Kopf Instruments) through 23 gauge metal guide tubes that reached
771 from the chamber grid to ~10-15 mm. dorsal to the hippocampus. Guide tubes were
772 placed at new locations at the beginning of each week and removed at the end of the
773 week after multiple days of recording. Neural signals were acquired, filtered,
774 amplified 1000x and digitized via the MAP Data Acquisition System (Plexon) at
775 40000 kHz resolution and sorted manually using a combination of offline sorter
776 (Plexon) and superparamagnetic clustering (Wave_Clus
777 http://www2.le.ac.uk/centres/csn/software)[48].

778 No attempt was made to pre-select neurons for any criterion other than the first
779 active cells that were encountered as the electrodes reached expected depths of the
780 dorsal extent of the hippocampus on a given day. Behavioral recordings started after
781 single units were isolated and could be held stably for at least 20 minutes. The 186
782 neurons we use in Figure 2 represent all units that were recorded during
783 presentation of at least 10 lure and 10 repeat trials with a minimum firing rate of
784 0.25 Hz. We used more stringent criteria for neuron selection for Figs. 3&4, as these
785 analyses are dependent on the sample size of the number of trials recorded for each
786 neuron. For Figure 3, we used the 137 neurons with at least 10 "lure"|lure and 10
787 "repeat"|repeat trials with at least a minimum firing rate of 0.25 Hz. For Figure 4, we
788 used the 76 neurons with at least 20 "lure"|lure and 20 "lure"|repeat trials and a
789 minimum firing rate of 0.5 Hz. In addition, for both of these figures, to calculate
790 firing rates during image presentation we measured spikes at an offset of 0.08 s
791 after image presentation (and image removal) to compensate for the latency of
792 visual stimuli to reach hippocampus [49,50]. Note that for both of these figures, we
793 empirically tested combinations of criteria close to each of these values (for
794 minimum trials, minimum firing rate and offset) via grid search and confirmed that
795 such small changes in these criteria did not appreciably change the statistics or our
796 conclusions.

797 Previous work has used a measure of population sparseness to indicate how many
798 neurons in a population respond to a given stimulus[28]. Since our task was
799 specifically designed to avoid conflation of short-term and long-term memory by

never showing the same images within or across sessions (the only images each monkey was shown more than once were novel images that became repeats, meaning they saw these images a total of twice), we cannot truly compare how our population of 137 neurons respond to the same stimulus. However, when we average the firing rate during all image periods for all neurons in our task and calculate population sparseness via the equation:

$$a^p = (\sum_{n=1}^{N} y_n / N)^2 / (\sum_{n=1}^{N} y_n{}^2) / N$$

where $y_n$ is the average firing rate for each neuron and N=137 total neurons, we get a value ($a^p$=0.37) similar to the population sparseness previously found in primate hippocampus ($a^p$=0.33,[24]). When we measured population sparseness this way for more specific image types, values were consistently between 0.36-0.37 (novel, $a^p$=0.37; lures, $a^p$=0.37; repeats, $a^p$=0.37; "lure"|lures, $a^p$=0.36; "repeat"|repeats, $a^p$=0.37; etc.). Therefore, our data indicate that population sparseness in this range is a general property of the firing distribution of CA3/DG neurons during image presentation regardless of the images shown.

**Population analysis:** For the initial analysis, the average firing rate for each neuron was measured during image presentation of each behaviorally-defined trial type (Fig. 1C). The average firing rate across neurons was then compared between trial types using multi-level ANOVA using the Matlab function anovan. The predictors were categorical variables for the three monkeys as well as the four trial types while the dependent variable was the average firing rate for each neuron during the respective condition.

The population spike count analysis was modeled after a recent publication on the responses of human hippocampal neurons to newly formed episodic memories[26]. First, we took only images that monkeys viewed for at least 400 ms so that we could measure the spike counts in the window from 200-500 ms after image presentation. This represented 61.4% of all images presented to the animals (Fig. 1B). We then took each image presentation period for each neuron and counted the spikes within this time period and divided by 300 ms to convert to Hz. (note that we did not use an offset for this analysis as in Figures 3&4 so we could best model the parameters of this recent publication. However, for the images we kept that were the shortest—those near 400 ms—counting spikes for 500 ms is close to the 80 ms offset we used in our other analyses). We normalized the firing rates for each neuron separately by pooling the fixation period firing rates during each session and z-scoring based on the mean and standard deviation of these (baseline) fixation firing rates for each neuron. This allowed us to pool z-scored firing rates across all neurons and then split them into separate groups for each trial type we wanted to compare: novel images (27614 trials), lure images (9671 trials) and repeat images (9178 trials). Quantile-quantile (Q-Q) plots were made using the Matlab qqplot function, which accounts for the different number of trials in both pools to give an equitable comparison of the firing distributions.

As evidenced by the skewed distributions of firing rates in Fig. 2A, firing rate spike counts do not have normal distributions (this was also confirmed by Kolmogorov-Smirnov Goodness-of-Fit test for normal distributions, $p<1E-100$; kstest in Matlab). In addition, the distributions for each of our firing rate counts had unequal variances (Bartlett test, $p<1E-100$; vartestn in Matlab). Therefore, we transformed the data to improve the normality and variances of the distributions for each trial type. We found a log transformation does a better job equalizing the variances than the untransformed data or square-root transformed data, as shown by the highest p-values for the Bartlett test[51]. For the log transformed and square-root transformed data, we added a constant value of 5 to each value in the original data to avoid negative numbers, since the minimum value in all 3 distributions was -4.9.

Once we transformed the distributions of firing rates for each of the three trial types, we performed a multi-level ANOVA on the transformed data to test for evidence of differences in the group means between the three distributions. The ANOVA—as well as the following ANOVAs for firing rates tested in this manuscript—is multi-level as we created categorical variables that labeled which of the three monkeys each spike count came from ("monkeys" variable) as well as which trial type each spike count came from ("trial_types" variable). These two categorical variables were then used to predict the vector of firing rates for all trials. This analysis creates three potential factors that could explain the variance in firing rates: differences between monkeys, differences between trial_types and differences between the interaction of monkeys X trial_types. We are interested in testing for differences between trial types after regressing out the variance from the other two factors. Therefore, p-values reported for each multi-level ANOVA test are for the trial type factor after inputting monkeys and trial_types as the categorical variables and the firing rates as the dependent variable using the Matlab function anovan.

Once we determined that there is evidence of differences between the group means between trial types, we tested for pairwise differences in the distributions using a two-sample Kolmogorov-Smirnov (K-S) test . Since we see evidence of differences between the novel v. lure and novel v. repeat distributions when visualized via QQ-plots (Fig. 2B), this test is ideal since it quantifies the similarity of two distributions using the absolute maximum distance from the x=y line in the QQ-plot. As we are doing three separate pairwise tests, the Bonferroni-corrected alpha in this case is 0.017.

**Single cell analyses:** For the analysis in Figure 3, we used the 137 neurons with at least 10 "lure"|lure and 10 "repeat"|repeat trials (using the single threshold version of the looking pattern assay, Fig. S7) with a minimum average firing rate during image presentations of 0.25 Hz. We found the firing rate during the presentation of images for each neuron by accumulating spikes from image on time to image off time and dividing by this length of time. We created vectors of these firing rates for each neuron using our behavioral methods to segregate the trials into pools of "lure"|lures and "repeat"|repeats. We also created vectors of novel images that matched the "lure"|lures (i.e., each of the novel images whose paired lure image was

correctly identified) and “repeat”|repeats (each of the novel images that was repeated and then correctly recognized). We then measured the Spearman correlation between the novel v. “lure”|lure firing rates as well as the novel v. “repeat”|repeat firing rates for each neuron (Figure 3A). To determine if these correlation values were significant, we utilized a permutation test method to account for the sparse firing structure of the data (instead of deriving a p-value from an assumed normal distribution). For example, if we have a neuron with 50 “lure”|lure firing rates, and therefore 50 novel image firing rates that pair with these lures, we pool all 100 firing rates together, shuffle them, randomly divide them into two surrogate vectors of 50 firing rates and find the correlation P’ between them. We then calculate 100,000 values of R’ by repeating this permutation process, and if the original P between “lure”|lures v. their respective novel images is greater than 95% of the surrogate P’ values, we consider the correlation significant. We performed this same process for the correlation values between “repeat”|repeats v. their respective novel images. Neurons that were significant only for “lure”|lures or “repeat”|repeats are shown in the top of Figure 3B, while neurons that were significant for neither are shown in the bottom.

For the analysis in Figure 4 we used only the 76 neurons recorded during at least 20 “lure”|lure trials, 20 “repeat”|repeat trials and with a minimum firing rate of 0.5 Hz. For each neuron, we found the change in firing rate (ΔFR) between each pair of novel and “lure”|lure images as well as for each pair of novel and “lure”|repeat images. Spikes were accumulated across the entire time the image was shown on screen and divided by this looking time to convert to Hz before subtracting between images to get ΔFR. We then found the **ρ** value from our looking pattern assay for each of these pairs of images (novel v. “lure”|lure and novel v. “lure”|repeat) and made separate scatterplots between ΔFR v. **ρ** for “lure”|lures and “lure”|repeats for each of our 76 neurons (example in Figure 4A). The Pearson correlations, which we call R, of each of these scatterplots are shown in Figure 4B. The median value of each is shown with a dashed line. Sign tests were done using the Matlab function signtest with the null hypothesis that the correlations come from a distribution with a median of 0. Comparisons between distributions were down using multi-level ANOVA, where the predictors were categorical variables labeling the monkey each neurons was from as well as the trial types being compared while the dependent variable was the correlation R of each scatterplot. In this case, we regressed out the variance from the monkey and monkey X trial_type variables such that we could specifically probe the effect of trial_type on R and therefore report the p-value of this test.

We fit the “lure”|lures, “lure”|repeat and “repeat”|repeat histograms in Fig. 4B with unimodal Gaussians using the Matlab function fit. The black line is a null distribution for visual effect with the average standard deviation of the other 3 histograms and centered at 0.

The R’ values in Figure 4D were calculated using a similar method as previous work that showed correlates of recognition in monkey hippocampus[15]. They are

comparable to the R values in Figure 4B-C, as they were found using graphs like Figure 4A but with percent change in looking time (ΔLT) as the abscissa instead of **ρ**. However, , we only kept repeat images when their associated novel image was ≥600 ms, and then only took those neurons recorded for at least 30 of these repeat images and with a fixation period firing rate≥0.5 Hz. This left 148 CA3/DG neurons, for which we found the Pearson correlation between the scatterplot of ΔFRs for each novel and repeat image pair v. ΔLT between the pairs (e.g., if the monkey looks at a novel image for 1 s. and its repeat for 0.5 s., this would be a -50% change in looking time). For this analysis, no offset was used (as in all other analyses) as the previous work this analysis was based on[15] accumulated spikes from 100 to 600 ms. after the time on for novel and repeat image presentation. Novel v. repeat comparisons with changes in looking times greater than 1000% or less than -1000% were removed as outliers so they did not overly influence the correlation. These trials represented only 0.05% of trials (only 5/148 neurons were recorded during such trials). The sign was flipped on the abscissa for each of these scatterplots such that negative values, which indicate better recognition memory, grow to the right[15]. Therefore, positive R' values indicate greater change in firing rate for better recognition memory. The sign test, Gaussian fits, significance of individual neurons and the multi-level ANOVA were performed as for Figure 4B-C as described above.

All data analyses were done in Matlab (The Mathworks) using custom scripts.

**Data availability:** The data and analysis code in support of the findings are available from the lead author on reasonable request.

**Acknowledgements:** We thank Craig Stark for helpful comments on a draft of the manuscript, John Wixted, Yuji Naya and Shih-pi Ku for helpful discussions, Arielle Tambini for pilot work on an early version of the project, Andrea Shang and Ellen Wang for assistance in animal training, Shohan Hasan for assistance in image collection and anonymous reviewers for suggestions to improve statistics. This work was supported by NIH grant MH084964.

**Author contributions:** J.J.S. performed research and analyzed data. J.J.S. and W.A.S. designed research and wrote the paper.

**Competing financial interests:** None.

# Population coding of pattern separation in the monkey hippocampus

John J. Sakon & Wendy A. Suzuki

Center for Neural Science. New York University. 4 Washington Place, New York, NY 10003.

Correspondence: john@cns.nyu.edu or wendy@cns.nyu.edu

## Supplementary Figures (S1-S9)

**Figure S1** Randomly selected example novel ("a") and lure ("b") image pairs.

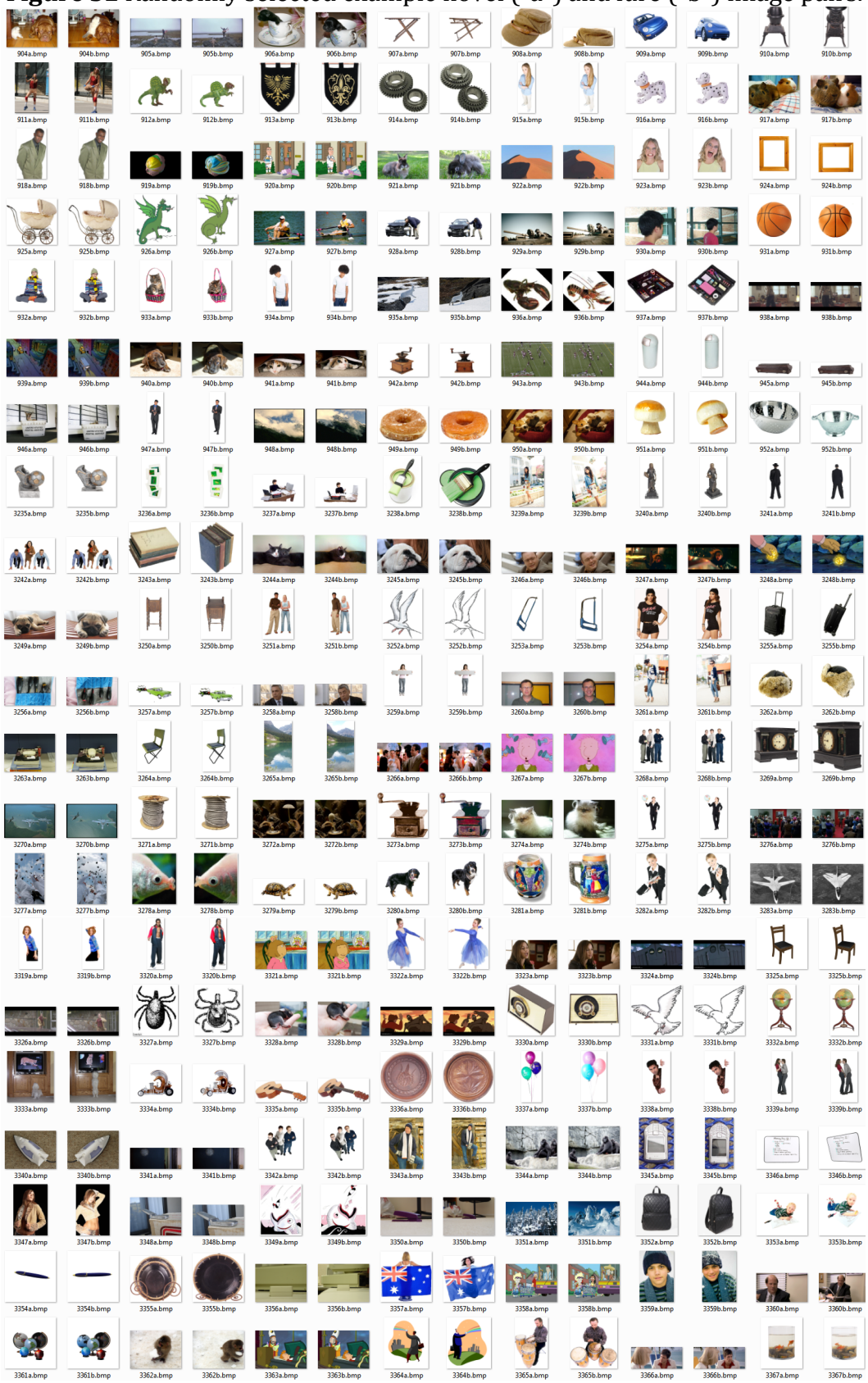

**Figure S2** Tests of behavioral performance. **A)** For the 62 recording sessions with at least 150 novel, 75 repeat and 75 lure images, we found the median looking time at each trial position to see if image looking times decrease during sessions (mean values had similar trends but are noisier due to outlier times). As shown, there is no decrease in looking times for lure (red) or repeat (blue) images, which maintain looking times around 600 and 500 ms, respectively. Novel image looking times decline after about 100 novel images were shown. Note that the 100$^{th}$ novel image would be the 250$^{th}$ trial shown in the average session (2/5 of total images shown are novel). The 250$^{th}$ trial in the average session would be where the 50$^{th}$ novel and lure images are shown (1/5 images are lures and 1/5 are repeats, with 1/5 foil images the remaining). Notably, even though there is a decline in looking times for novel images after the 100$^{th}$ novel image is shown, there is no concomitant decrease in looking times for lure or repeat trials after the 50$^{th}$ trial is shown. **B)** We pooled all trials for each classified trial type across sessions and asked if monkeys were better at recognizing lure and repeat images when there were less intervening stimuli between the novel and lure or novel and repeat image. The range of intervening stimuli between each lure or repeat pair was between 0 and 3. Our expectation would be that "lure"|lures and "repeat"|repeats (that is, successfully identified lures and repeats) should on average have less intervening stimuli. This was not the case, as the average number of intervening stimuli for each trial type was not statistically different whether using looking times (p=0.82, multi-level ANOVA) or **C)** the looking pattern assay (p=0.63, multi-level ANOVA) to classify trials. Each of the multi-level ANOVAs used categorical variables for the three monkeys and the four classified trial types as predictors with the number of intervening stimuli for each trial as the dependent variable. P-values represent the trial type factors after regressing out the variance between monkeys and the interaction between monkeys and trial types.

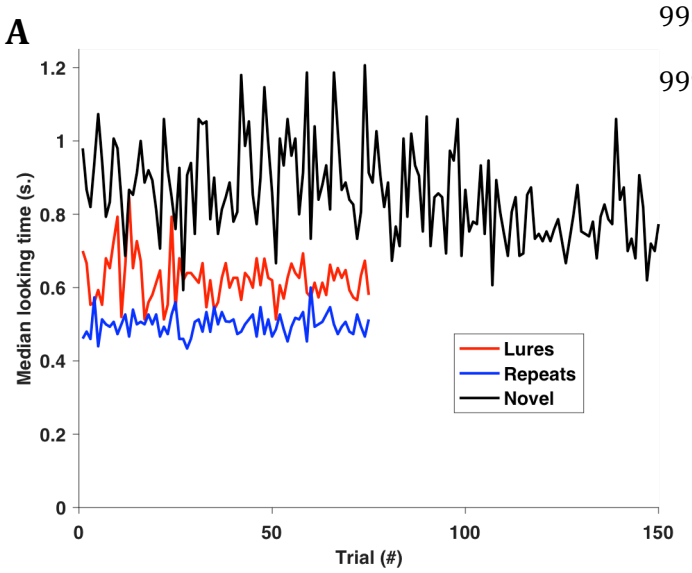

1000

1001

**B**

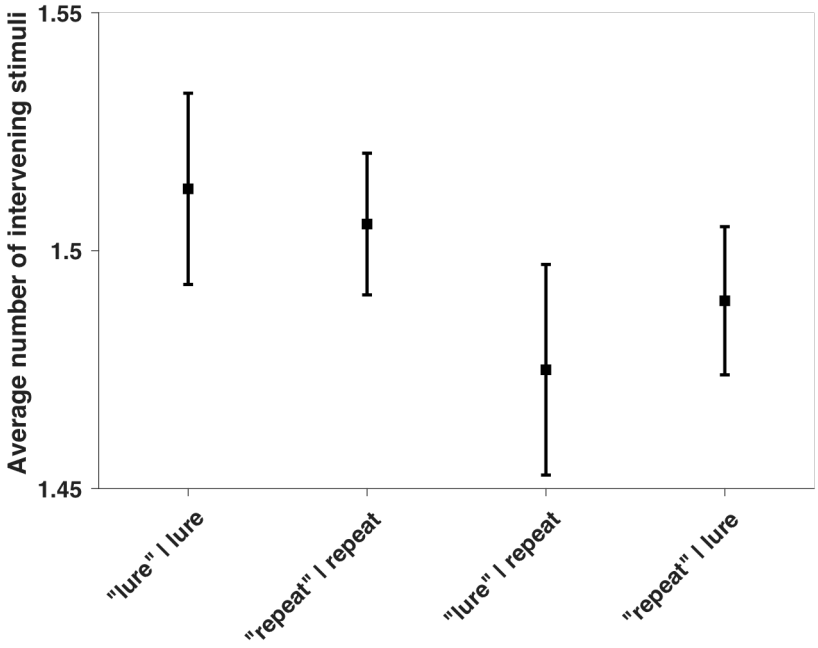
1.55
1.5
1.45
Average number of intervening stimuli
"lure" | lure
"repeat" | repeat
"lure" | repeat
"repeat" | lure

**C**

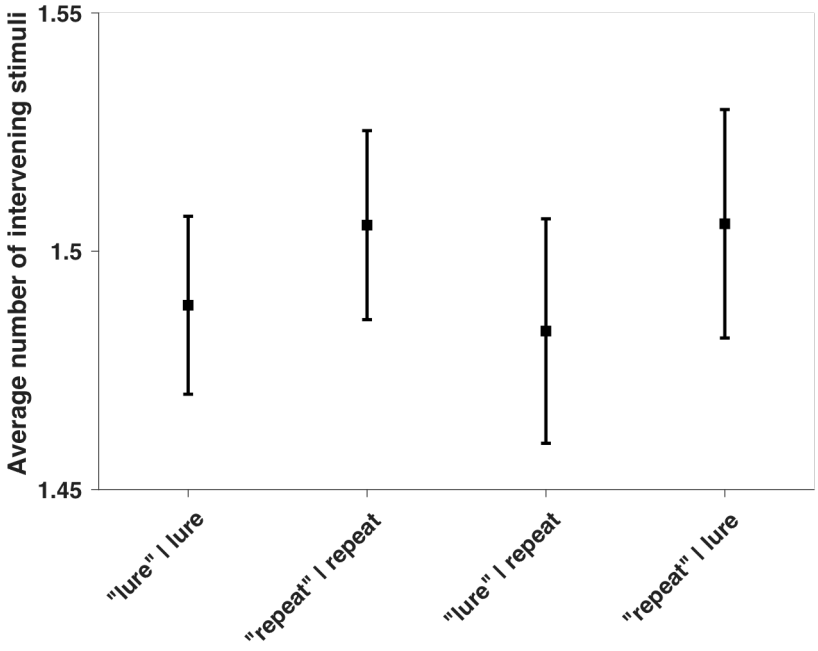
1.55
1.5
1.45
Average number of intervening stimuli
"lure" | lure
"repeat" | repeat
"lure" | repeat
"repeat" | lure

**Figure S3** Example images and Gaussian kernel fills for looking pattern analysis. Fixation points were found using ClusterFix [18]. Gaussian kernels were added at each detected fixation point and the concatenated rows of the heat maps (bottom images) were correlated to get a single measure of similarity, **ρ**, between the images.

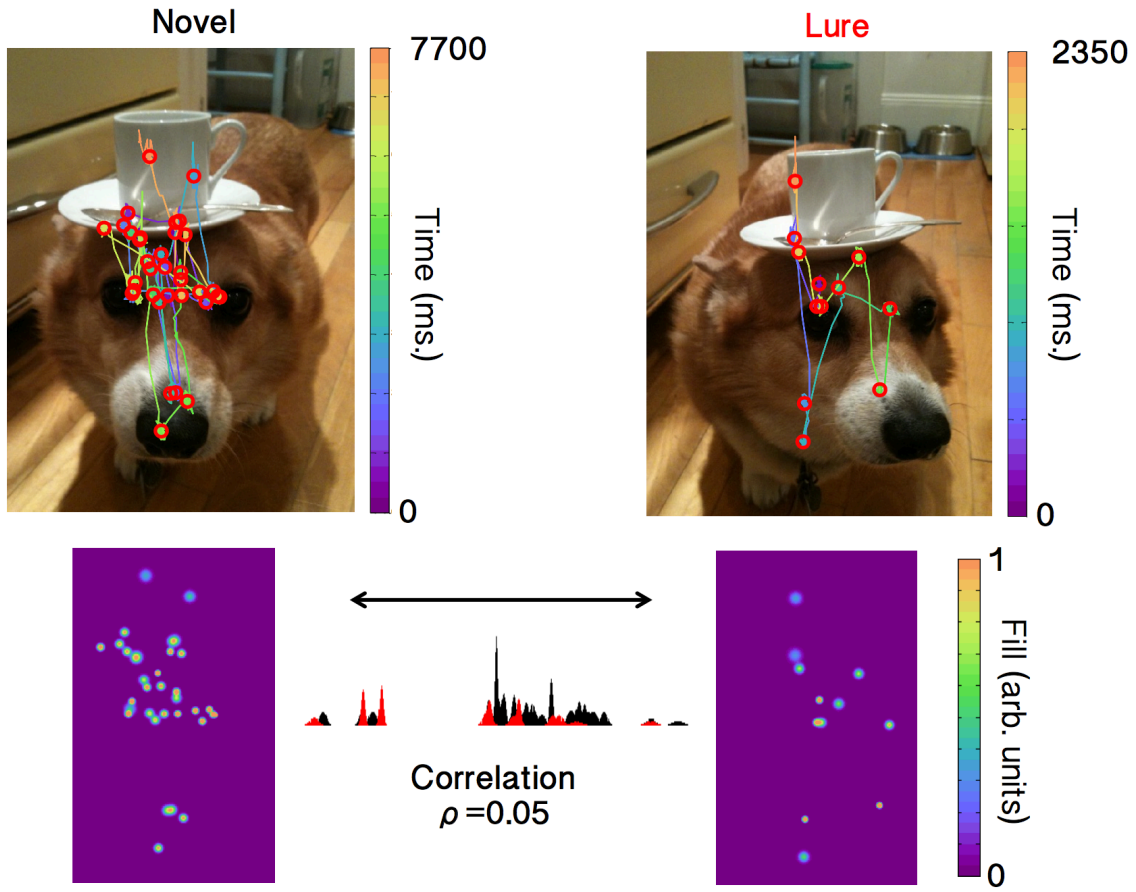

**Figure S4** (Top) 3-dimensional view of recording locations from monkey I. Left to right shows the posterior to anterior direction, with colors from black to white indicating 6 to 14 mm. anterior of ear bars. (Bottom) Same outline as in top figure superimposed over sagittal MRI slice 13 mm. right of midline.

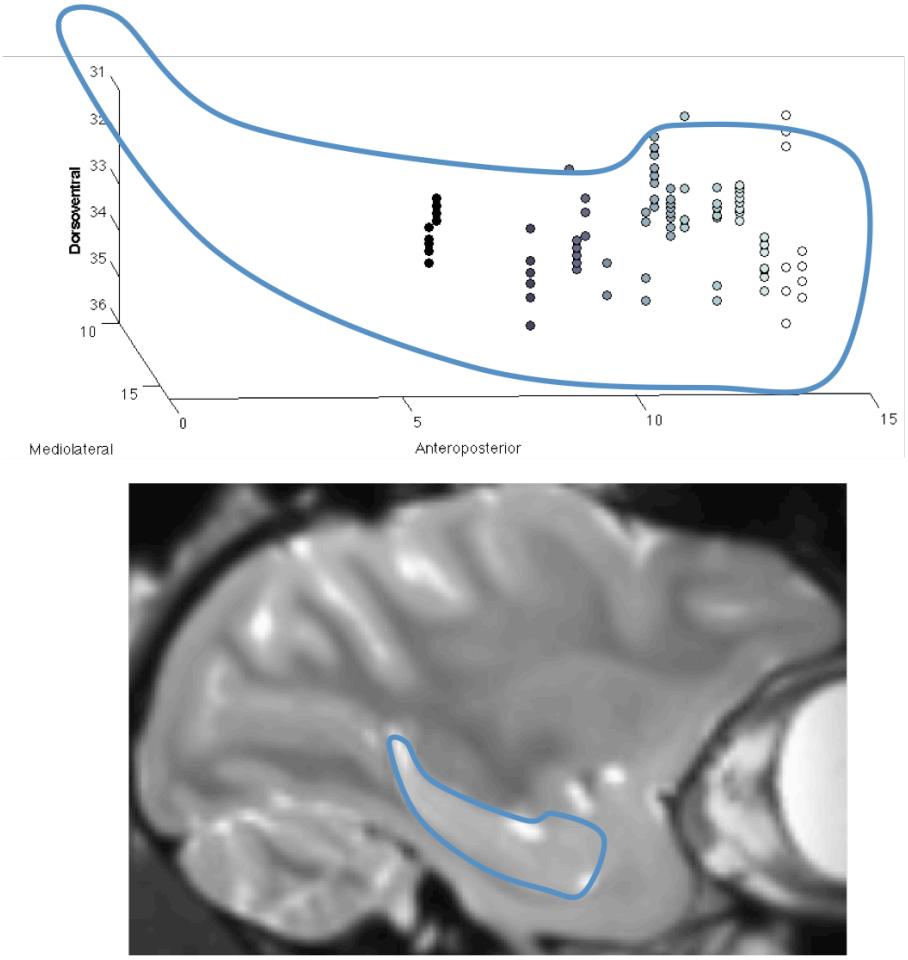

**Figure S5** Monkey I coronal slices at 3 anteroposterior levels of hippocampus with recording sites superimposed on estimated recording locations (dots). Slices are aligned in the mediolateral direction. Distance is relative to ear bars = 0 mm.

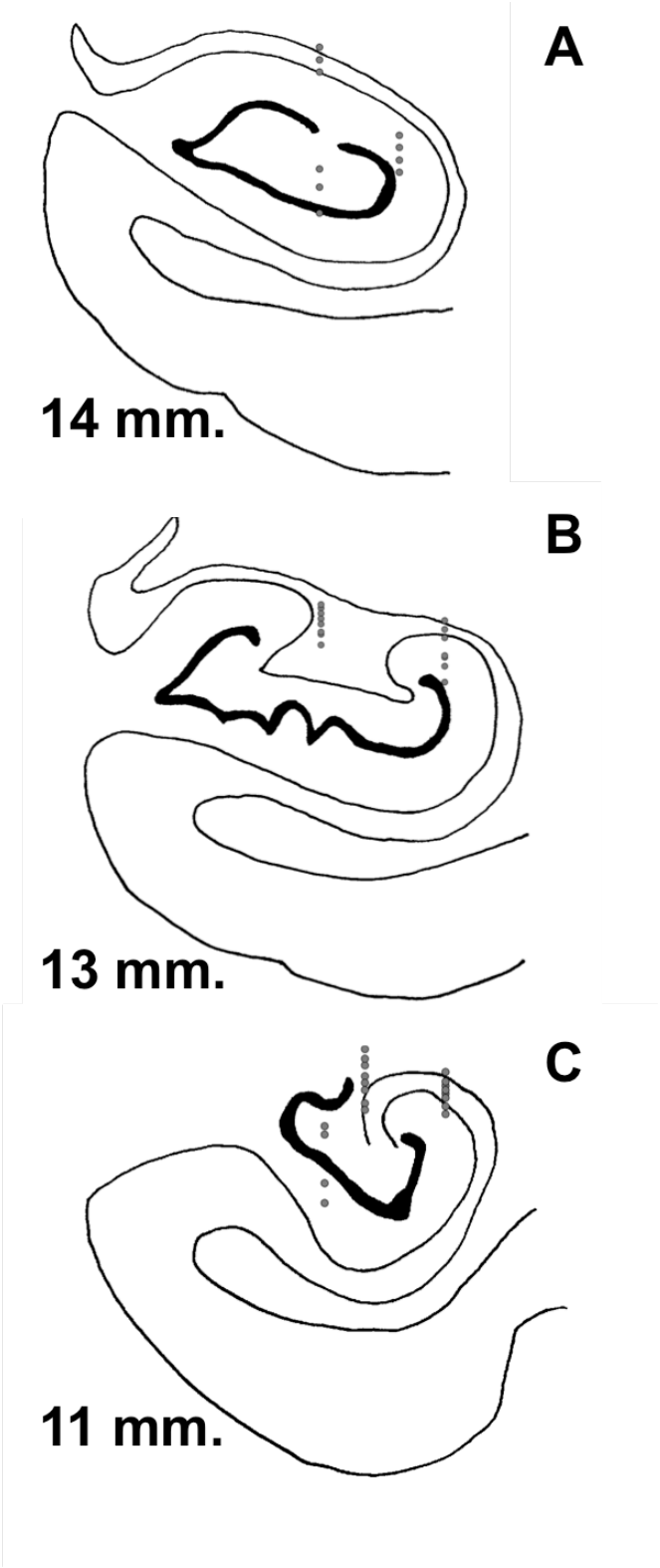

**Figure S6** Plot details as in Fig. 2, but using behavior to classify trials. Lures are now "lure"|lures in this figure, and repeats are now "repeat"|repeats. Notice that for all normalized firing rates ≥ 0 there are proportionally more "lure"|lure than "repeat"|repeat trials, while for all normalized firing rates < 0 there are proportionally more "repeat"|repeat trials than "lure"|lure trials. The distribution of firing rates for these three trial types are significantly different (p=0.018, multi-level ANOVA).

For the QQ plot (right), the deviance between the lure and repeat distributions begins at the 90% quantile near a normalized firing rate of 2. As in Figure 2, novel and "lure"|lure trials are not significantly different (p=0.36, Kolmogorov-Smirnov test), while both novel v. "repeat"|repeat (p=3.1E-5) and "lure"|lure v. "repeat"|repeat (p=1.7E-6) show significantly different distributions. Counts of each trial type: novel = 11777 trials, "lure"|lure = 4293 trials, "repeat"|repeat = 3064 trials. Only trials from  neurons with at least 20 of each of these trial types and a minimum average firing rate of 0.5 Hz. were pooled for this analysis.

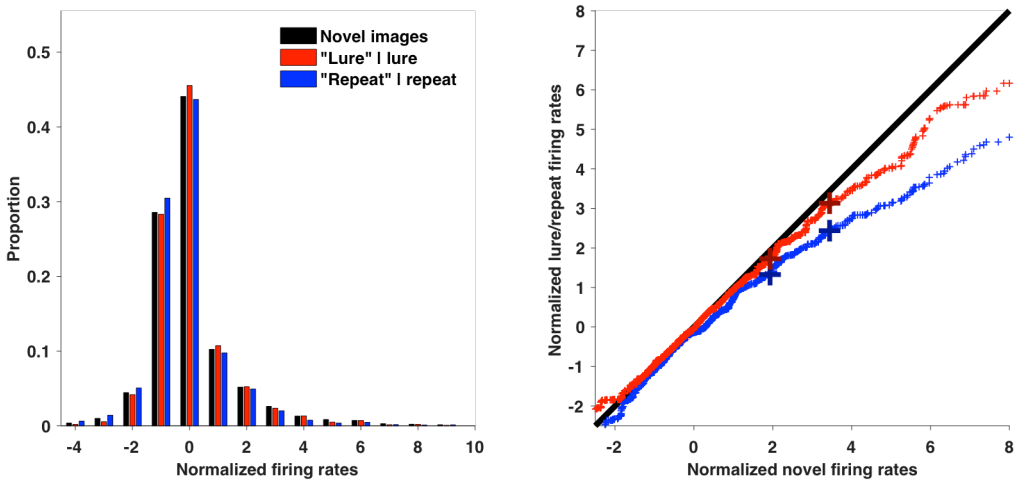

**Figure S7** Looking pattern assay classification performance using a single threshold (**ρ** = 0.6) vs. using the best threshold for each session. As explained in Methods, we use a single threshold in our looking pattern assay for the analysis in Figure 3 in order to more selectively classify "repeat"|repeat trials while not sacrificing as much selectively of "lure"|lure trials. The classification results for a single threshold are shown at left, with 59% of repeats classified as "lure"|repeat (blue). The corollary of this classification is that only 41% of repeats are classified as "repeat"|repeat. This is in contrast to the looking pattern assay using the best threshold as shown at right (same data as in the center graph of Fig. 1D), where 40% of repeats are classified as "lure"|repeat (blue) and therefore 60% of repeats are classified as "repeat"|repeat. In effect, using a single threshold allows us to be choosier for which trials we consider successful recognition by the monkey: only 41% as opposed to 60% of all repeats. "Lure"|lure trials (red) do not show as much of a change in classification between these two methods, with 70% of lure trials using a single threshold (left) v. 62% of lure trials when using the best threshold for each session (right).

However, note that results show similar trends in this same analysis even when using the best threshold for each session (Fig. S8).

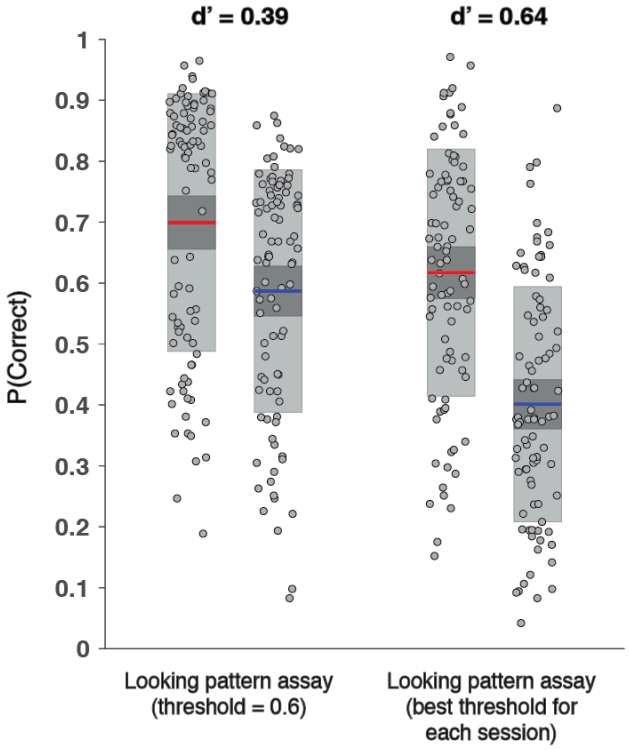

**Figure S8** Figure details as in Figure 3B. **A)** All lure and all repeat trials used instead of using behavior to classify "lure"|lure and "repeat"|repeat trials. The subpopulation of neurons significant for lures shows a trend towards being larger than the subpopulation significant for repeats (p=0.17, $\chi^2$ (1.92,1)). **B)** Trial classification using the looking pattern assay using best threshold as opposed to a single threshold for **ρ**. As explained in methods, a single threshold was used for the analysis in Figure 3B for more strict selection of "repeat"|repeat trials. The subpopulation of neurons significant for lures shows a trend towards being larger than the subpopulation significant for repeats (p=0.12, $\chi^2$ (2.46,1)).

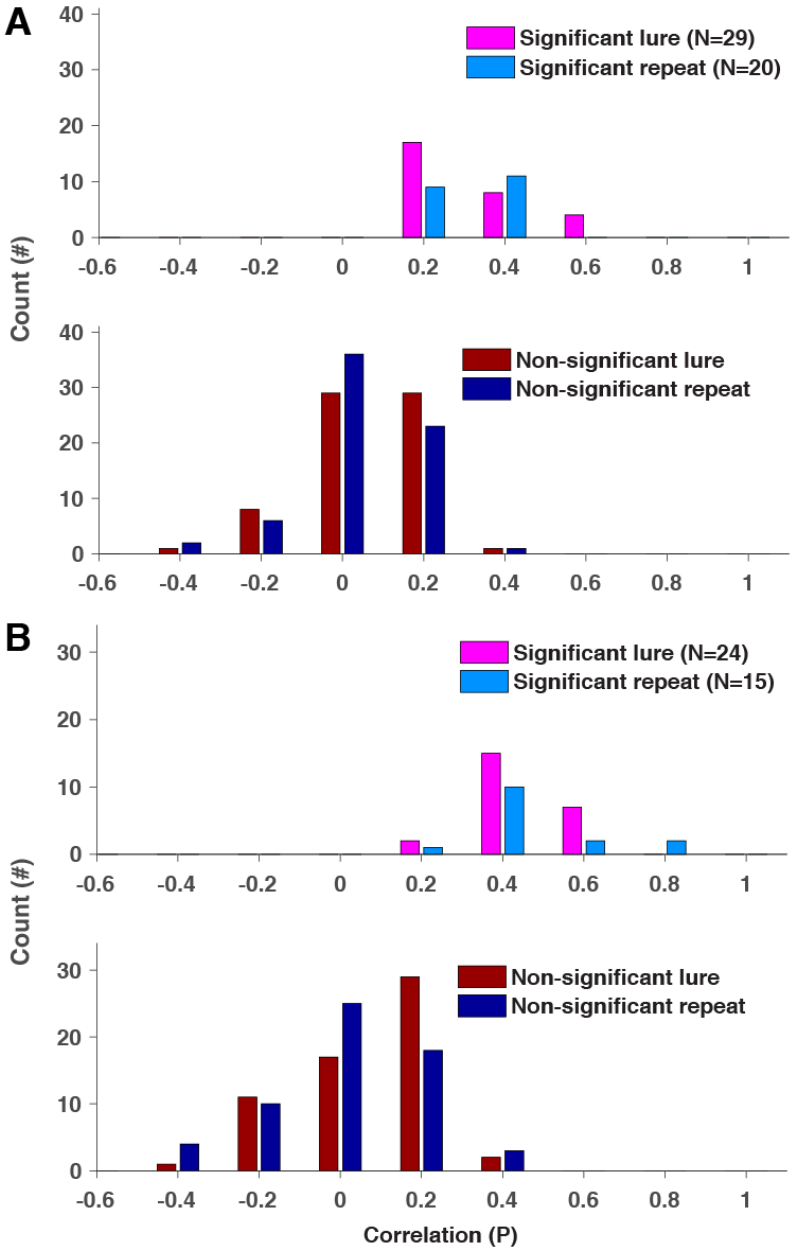

**Figure S9** (Left) Linear fits of the "lure"|lure trials for the 16/76 neurons with significant correlations ($p<0.05$). Each fit is of the data for a single neuron as in Fig. 4A. The red line is the average of these 16 neurons. (Right) The same 16 neurons with linear fits shown for "lure"|repeat trials. The blue line is the average. 3/16 of the correlations to "lure"|repeats were significant while 10/16 had a positive slope.

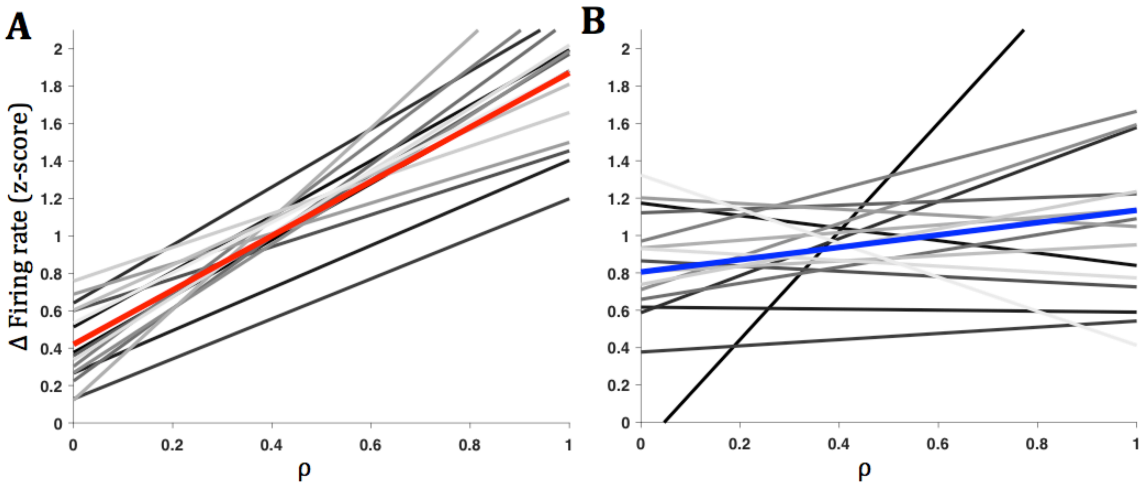

## References:


1 Hunsaker, M. R. & Kesner, R. P. The operation of pattern separation and pattern completion processes associated with different attributes or domains of memory. *Neurosci Biobehav R* **37**, 36-58, doi:DOI 10.1016/j.neubiorev.2012.09.014 (2013).

2 Leutgeb, S. & Leutgeb, J. K. Pattern separation, pattern completion, and new neuronal codes within a continuous CA3 map. *Learn Memory* **14**, 745-757, doi:10.1101/lm.703907 (2007).

3 Bakker, A., Kirwan, C. B., Miller, M. & Stark, C. E. L. Pattern separation in the human hippocampal CA3 and dentate gyrus. *Science* **319**, 1640-1642, doi:DOI 10.1126/science.1152882 (2008).

4 Berron, D. *et al.* Strong Evidence for Pattern Separation in Human Dentate Gyrus. *The Journal of Neuroscience* **36**, 7569-7579, doi:10.1523/jneurosci.0518-16.2016 (2016).

5 Kirwan, C. B. & Stark, C. E. Overcoming interference: an fMRI investigation of pattern separation in the medial temporal lobe. *Learn Mem* **14**, 625-633, doi:10.1101/lm.663507 (2007).

6 Lacy, J. W., Yassa, M. A., Stark, S. M., Muftuler, L. T. & Stark, C. E. L. Distinct pattern separation related transfer functions in human CA3/dentate and CA1 revealed using high-resolution fMRI and variable mnemonic similarity. *Learn Memory* **18**, 15-18, doi:10.1101/lm.1971110 (2011).

7 Suthana, N. A. *et al.* Specific responses of human hippocampal neurons are associated with better memory. *P Natl Acad Sci USA* **112**, 10503-10508, doi:10.1073/pnas.1423036112 (2015).

8 Guzowski, J. F., Knierim, J. J. & Moser, E. I. Ensemble dynamics of hippocampal regions CA3 and CA1. *Neuron* **44**, 581-584, doi:Doi 10.1016/J.Neuron.2004.11.003 (2004).

9 Leutgeb, J. K., Leutgeb, S., Moser, M. B. & Moser, E. I. Pattern separation in the dentate gyrus and CA3 of the hippocampus. *Science* **315**, 961-966, doi:DOI 10.1126/science.1135801 (2007).

10 Leutgeb, S., Leutgeb, J. K., Treves, A., Moser, M. B. & Moser, E. I. Distinct ensemble codes in hippocampal areas CA3 and CA1. *Science* **305**, 1295-1298, doi:10.1126/science.1100265 (2004).

11 Neunuebel, J. P. & Knierim, J. J. CA3 retrieves coherent representations from degraded input: direct evidence for CA3 pattern completion and dentate gyrus pattern separation. *Neuron* **81**, 416-427, doi:10.1016/j.neuron.2013.11.017 (2014).

12 Vazdarjanova, A. & Guzowski, J. F. Differences in hippocampal neuronal population responses to modifications of an environmental context: Evidence for distinct, yet complementary, functions of CA3 and CA1 ensembles. *J Neurosci* **24**, 6489-6496, doi:10.1523/JNEUROSCI.0350-04.2004 (2004).

13 Logothetis, N. K., Pauls, J., Augath, M., Trinath, T. & Oeltermann, A. Neurophysiological investigation of the basis of the fMRI signal. *Nature* **412**, 150-157, doi:10.1038/35084005 (2001).

14 Kim, J. & Yassa, M. A. Assessing recollection and familiarity of similar lures in a behavioral pattern separation task. *Hippocampus* **23**, 287-294, doi:10.1002/hipo.22087 (2013).

15 Jutras, M. J. & Buffalo, E. A. Recognition memory signals in the macaque hippocampus. *P Natl Acad Sci USA* **107**, 401-406 (2010).

16 Spelke, E. S. in *Measurement of audition and vision in the first year of life.* (ed G. Gottlieb & N. Krasnegor) 323-363 (Ablex, 1985).

17 Holmqvist, K., Nyström, N., Andersson, R., Dewhurst, R., Jarodzka, H., & Van de Weijer, J. in *Eye Tracking: A comprehensive guide to methods and measures* (ed K. Holmqvist) (Oxford University Press, 2010).

18 Konig, S. D. & Buffalo, E. A. A nonparametric method for detecting fixations and saccades using cluster analysis: Removing the need for arbitrary thresholds. *J Neurosci Meth* **227**, 121-131, doi:10.1016/j.jneumeth.2014.01.032 (2014).

19 Hannula, D. E. & Ranganath, C. The Eyes Have It: Hippocampal Activity Predicts Expression of Memory in Eye Movements. *Neuron* **63**, 592-599, doi:10.1016/j.neuron.2009.08.025 (2009).

20 Smith, C. N. & Squire, L. R. Experience-Dependent Eye Movements Reflect Hippocampus-Dependent (Aware) Memory. *J Neurosci* **28**, 12825-12833, doi:10.1523/JNEUROSCI.4542-08.2008 (2008).

21 Foulsham, T. *et al.* Comparing scanpaths during scene encoding and recognition: A multi-dimensional approach. *J Eye Movement Res* **5** (2012).

22 Foulsham, T. & Underwood, G. What can saliency models predict about eye movements? Spatial and sequential aspects of fixations during encoding and recognition. *Journal of vision* **8** (2008).

23 Frank, L. M., Brown, E. N. & Wilson, M. A. A comparison of the firing properties of putative excitatory and inhibitory neurons from CA1 and the entorhinal cortex. *J Neurophysiol* **86**, 2029-2040 (2001).

24 Rolls, E. T. & Treves, A. The neuronal encoding of information in the brain. *Prog Neurobiol* **95**, 448-490, doi:10.1016/j.pneurobio.2011.08.002 (2011).

25 Saleem, K. S. & Logothetis, N. K. *A combined MRI and histology atlas of the rhesus monkey brain in stereotaxic coordinates*. 2nd edn, (Academic Press, 2012).

26 Wixted, J. T. *et al.* Sparse and distributed coding of episodic memory in neurons of the human hippocampus. *P Natl Acad Sci USA* **111**, 9621-9626, doi:DOI 10.1073/pnas.1408365111 (2014).

27 Heeger, D. J. & Ress, D. What does fMRI tell us about neuronal activity? *Nat Rev Neurosci* **3**, 142-151, doi:10.1038/nrn730 (2002).

28 Rolls, E. T. Pattern separation, completion, and categorisation in the hippocampus and neocortex. *Neurobiol Learn Mem* **129**, 4-28, doi:10.1016/j.nlm.2015.07.008 (2016).

29 Dudukovic, N. M., Preston, A. R., Archie, J. J., Glover, G. H. & Wagner, A. D. High-resolution fMRI Reveals Match Enhancement and Attentional Modulation in the Human Medial Temporal Lobe. *J Cognitive Neurosci* **23**, 670-682, doi:Doi 10.1162/Jocn.2010.21509 (2011).

30 Stark, C. E. L. & Squire, L. R. Functional magnetic resonance imaging (fMRI) activity in the hippocampal region during recognition memory. *J Neurosci* **20**, 7776-7781 (2000).

31 Fried, I., MacDonald, K. A. & Wilson, C. L. Single neuron activity in human hippocampus and amygdala during recognition of faces and objects. *Neuron* **18**, 753-765, doi:Doi 10.1016/S0896-6273(00)80315-3 (1997).

32 Merkow, M. B., Burke, J. F. & Kahana, M. J. The human hippocampus contributes to both the recollection and familiarity components of recognition memory. *P Natl Acad Sci USA* **Early Edition** (2015).

33 Rutishauser, U., Mamelak, A. N. & Schuman, E. M. Single-trial learning of novel stimuli by individual neurons of the human hippocampus-amygdala complex. *Neuron* **49**, 805-813, doi:10.1016/j.neuron.2006.02.015 (2006).

34 Rutishauser, U., Schuman, E. M. & Mamelak, A. N. Activity of human hippocampal and amygdala neurons during retrieval of declarative memories. *Proc Natl Acad Sci U S A* **105**, 329-334, doi:10.1073/pnas.0706015105 (2008).

35 Quiroga, R. Q. Concept cells: the building blocks of declarative memory functions. *Nat Rev Neurosci* **13**, 587-597, doi:Doi 10.1038/Nrn3251 (2012).

36 Brun, V. H. *et al.* Place cells and place recognition maintained by direct entorhinal-hippocampal circuitry. *Science* **296**, 2243-2246, doi:Doi 10.1126/Science.1071089 (2002).

37 Dimsdale-Zucker, H. R., Ritchey, M., Ekstrom, A. D., Yonelinas, A. P. & Ranganath, C. CA1 And CA3 Differentially Support Spontaneous Retrieval Of Episodic Contexts Within Human Hippocampal Subfields. *bioRxiv*, doi:10.1101/142349 (2017).

38 Nakazawa, K. Dentate Mossy Cell and Pattern Separation (vol 93, pg 465, 2017). *Neuron* **93**, 1236-1236, doi:10.1016/j.neuron.2017.02.024 (2017).

39 Aronov, D., Nevers, R. & Tank, D. W. Mapping of a non-spatial dimension by the hippocampal-entorhinal circuit. *Nature* **543**, 719-722, doi:10.1038/nature21692 (2017).

40 Waydo, S., Kraskov, A., Quiroga, R. Q., Fried, I. & Koch, C. Sparse representation in the human medial temporal lobe. *J Neurosci* **26**, 10232-10234, doi:Doi 10.1523/Jneurosci.2101-06.2006 (2006).

41 Dragoi, G. & Tonegawa, S. Preplay of future place cell sequences by hippocampal cellular assemblies. *Nature* **469**, 397-401, doi:Doi 10.1038/Nature09633 (2011).

42 Savarese, S. & Fei-Fei, L. 3D generic object categorization, localization and pose estimation. *Ieee I Conf Comp Vis*, 1245-1252 (2007).

43 Thomaz, C. E. & Giraldi, G. A. A new ranking method for principal components analysis and its application to face image analysis. *Image Vision Comput* **28**, 902-913, doi:10.1016/j.imavis.2009.11.005 (2010).

44 Li, L. J. & Fei-Fei, L. What, where and who? Classifying events by scene and object recognition. *Ieee I Conf Comp Vis*, 345-+ (2007).

45 Russakovsky, O. *et al.* ImageNet Large Scale Visual Recognition Challenge. *Int J Comput Vision* **115**, 211-252, doi:10.1007/s11263-015-0816-y (2015).

46 Fischer, B. & Boch, R. Saccadic eye movements after extremely short reaction times in the monkey. *Brain Res* **260**, 21-26 (1983).

47 Dorr, M., Martinetz, T., Gegenfurtner, K. R. & Barth, E. Variability of eye movements when viewing dynamic natural scenes. *Journal of vision* **10**, 28, doi:10.1167/10.10.28 (2010).

48 Quiroga, R. Q., Nadasdy, Z. & Ben-Shaul, Y. Unsupervised spike detection and sorting with wavelets and superparamagnetic clustering. *Neural Comput* **16**, 1661-1687 (2004).

49 Naya, Y. & Suzuki, W. A. Integrating What and When Across the Primate Medial Temporal Lobe. *Science* **333**, 773-776 (2011).

50 Rey, H. G., Fried, I. & Quiroga, R. Q. Timing of Single-Neuron and Local Field Potential Responses in the Human Medial Temporal Lobe. *Curr Biol* **24**, 299-304, doi:10.1016/j.cub.2013.12.004 (2014).

51 MacDonald, J. H. *Handbook of Biological Statistics*. 3rd edn, 137-139 (Sparky House Publishing, Baltimore, Maryland, 2014).